# *Hbb* vertex at four loops and hard matching coefficients in SCET for various currents

Amlan Chakraborty,[1,2] Tobias Huber,[3] Roman N. Lee,[4] Andreas von Manteuffel,[1] Robert M. Schabinger,[1] Alexander V. Smirnov,[5,6] Vladimir A. Smirnov,[7,6] and Matthias Steinhauser[8]

[1]*Department of Physics and Astronomy, Michigan State University, East Lansing, Michigan 48824, USA*
[2]*The Institute of Mathematical Sciences, HBNI, Taramani, Chennai 600113, India*
[3]*Naturwissenschaftlich-Technische Fakultät, Universität Siegen, Walter-Flex-Straße 3, 57068 Siegen, Germany*
[4]*Budker Institute of Nuclear Physics, 630090 Novosibirsk, Russia*
[5]*Research Computing Center, Moscow State University, 119991 Moscow, Russia*
[6]*Moscow Center for Fundamental and Applied Mathematics, 119992 Moscow, Russia*
[7]*Skobeltsyn Institute of Nuclear Physics of Moscow State University, 119991 Moscow, Russia*
[8]*Institut für Theoretische Teilchenphysik, Karlsruhe Institute of Technology (KIT), 76128 Karlsruhe, Germany*

(Received 20 May 2022; accepted 8 July 2022; published 13 October 2022)

We compute the four-loop corrections to the Higgs-bottom vertex within massless QCD and present analytic results for all color structures. The infrared poles of the renormalized form factor agree with the predicted four-loop pattern. Furthermore, we use the results for the Higgs-bottom, photon-quark, and Higgs-gluon form factors to provide hard matching coefficients in soft-collinear effective theory up to four-loop accuracy.

DOI: 10.1103/PhysRevD.106.074009

## I. INTRODUCTION

In the next decade the Higgs boson will play a central role in many of the analyses performed with data taken at the general purpose experiments ATLAS and CMS at the Large Hadron Collider (LHC) at CERN. Improved analysis tools will increase the precision of observables, motivating new calculations on the theory side in order to match the uncertainties of the experiments.

The dominant channel for Higgs boson production is via gluon fusion. Although in the Standard Model (SM) the contribution from bottom quark annihilation is only at the percent level, it might be important in extended models with an enhanced coupling of the Higgs boson to bottom quarks. In the SM, state-of-the-art for the inclusive production rate $b\bar{b} \to H + X$, with $X$ being any hadronic state, is next-to-next-to-next-to-leading order (N$^3$LO) [1,2] (see Refs. [3–5] for the NNLO corrections and [6] for the next-to-next-to-next-to-leading logarithmic resummation). An important ingredient in the analysis of Ref. [2] is the three-loop Higgs-bottom form factor which has been computed in Ref. [7] and cross-checked in Refs. [1,8]. In this work we provide results for the four-loop corrections to the Higgs-bottom form factor, which constitutes a building block for the Higgs boson production cross section and the differential rate of Higgs boson decays to bottom quarks at N$^4$LO.

There are two different ways to view Higgs boson production in bottom-antibottom quark annihilation. In the so-called five-flavor scheme, the bottom quark is considered as a massless parton which is part of the proton. In the four-flavor scheme, the first step is the production of two (massive) bottom and antibottom quark pairs via gluon splitting. Afterwards a bottom and an antibottom quark annihilate to produce the Higgs boson. From the technical point of view the four-flavor scheme is more involved and, in fact, in this approach only NLO corrections are available [9–12], which are of the same order in the strong coupling as the N$^3$LO corrections available in the five-flavou scheme [1,2].

An attractive framework to describe high-energy cross sections is based on soft-collinear effective theory (SCET) [13–19], which can be used to separate the various scales present in a process and to perform a resummation of potentially large logarithms. The matching of SCET to QCD is achieved with the help of so-called hard matching coefficients that can be extracted from the massless form factors computed in QCD. In this work, we calculate matching coefficients from results for the four-loop $Hb\bar{b}$, $\gamma^* q\bar{q}$, and $Hgg$ form factors. An important aspect of this derivation is an explicit check of the prediction [20–32] for the infrared poles of the renormalized $Hb\bar{b}$ form factor using recent analytical results for the four-loop cusp [33–36] and quark collinear [36,37] anomalous dimensions.

The outline of the paper is as follows. In Sec. II, we discuss the bare Higgs-bottom form factor and present our result for the four-loop term. For the Higgs-bottom, photon-quark, and Higgs-gluon form factors, we discuss the ultraviolet (UV) renormalization in Sec. III and the infrared (IR) subtractions in Sec. IV. The SCET hard matching coefficients for all three form factors are presented in Sec. V. We conclude in Sec. VI.

## II. THE $Hb\bar{b}$ FORM FACTOR AT FOUR LOOPS

We define the Higgs-bottom form factor via

$$\mathcal{F}_b(q^2) = -\frac{1}{2q^2}\mathrm{Tr}(\not{q}_2\Gamma_b\not{q}_1), \tag{1}$$

where $\Gamma_b$ is the Higgs-bottom vertex function, $q_1$ and $q_2$ are the incoming quark and antiquark momenta, and $q = q_1 + q_2$ is the momentum of the Higgs boson. Sample Feynman diagrams contributing to $F_b$ at the four-loop level are shown in Fig. 1. We employ conventional dimensional regularization to regularize UV and IR divergences, and for the number of spacetime dimensions $d$ we use $d = 4 - 2\epsilon$. Two- and three-loop corrections to $F_b$ have been computed in Refs. [38,7], respectively. The extension of the three-loop result up to order $\epsilon^2$ and the four-loop results with two and three closed fermion loops have been computed in [8]. In this work we complete the four-loop corrections by computing the contributions of all remaining color factors.

The bare form factor is conveniently parametrized in terms of the bare strong coupling constant and the bare Yukawa coupling $y_0 = m_{b,0}/v$ where $m_{b,0}$ and $v$ are the bare bottom quark mass and Higgs vacuum expectation value. The perturbative expansion of this bare form factor reads

$$\mathcal{F}_b = y_0\left[1 + \sum_{n\geq 1} a_0^n \left(\frac{\mu_0^2}{-q^2 - i0}\right)^{n\epsilon} S_\epsilon^n F_b^{(n)}\right], \tag{2}$$

where

$$S_\epsilon = e^{-\epsilon\gamma}(4\pi)^\epsilon, \qquad a_0 = \frac{\alpha_s^0}{4\pi}, \tag{3}$$

$\alpha_s^0$ is the bare strong coupling, $\mu_0$ is the 't Hooft scale, $\gamma \approx 0.577216$ is Euler's constant, and the $-i0$ description fixes the branch cut ambiguity for $q^2 > 0$. We stress that we keep a nonzero bottom mass only in the Yukawa coupling and treat the bottom quark as a massless particle otherwise. $F_b^{(n)}$ develops poles up to $1/\epsilon^{2n}$. However, nontrivial information specific to some loop order is contained only in the $1/\epsilon^2$ poles and higher order $\epsilon$ terms. All higher poles, $1/\epsilon^{2n}, \ldots, 1/\epsilon^3$, are fixed from the lower-loop contributions. In fact, the $1/\epsilon^2$ poles are determined by the (universal) cusp anomalous dimension, and the $1/\epsilon$ poles are determined by the collinear anomalous dimension.

We generate the Feynman diagrams with Qgraf [39] and employ FORM 4 [40] to express the form factor in terms of unreduced scalar Feynman integrals. For the color algebra we use COLOR.H [41], which conveniently produces a result that is valid for a general simple Lie algebra. We find the color structures listed in Fig. 1, where $C_R$ is the quadratic Casimir operator and $d_R^{abcd}$ is the fully symmetrical tensor originating from the trace over four generators, with $R = F, A$ for the fundamental and adjoint representation, respectively. Further, $N_F$ is the dimension of the fundamental representation and $n_f$ is the number of light quarks. For a $SU(N_c)$ gauge group the relevant invariants or color factors read

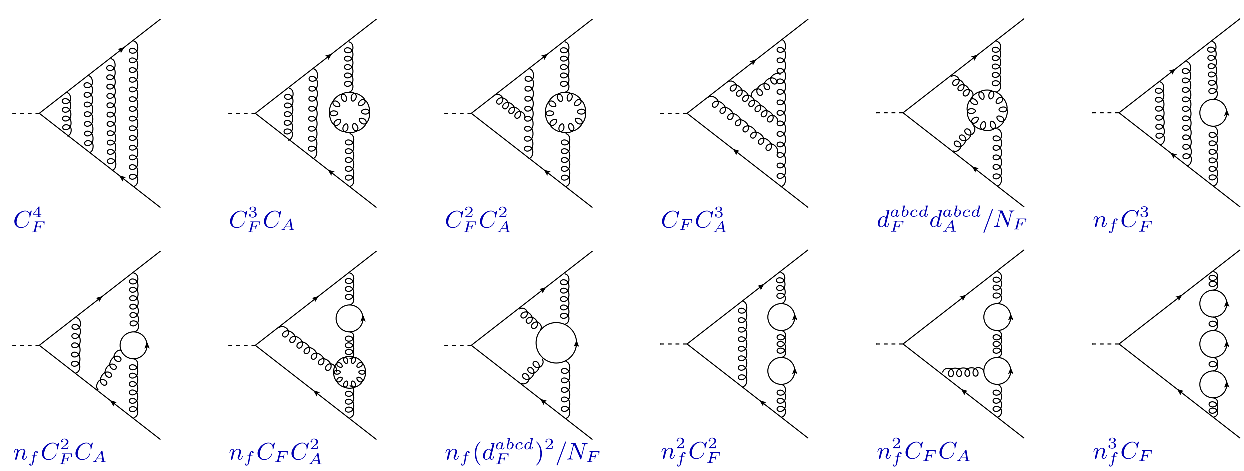


FIG. 1. Sample Feynman diagrams contributing to the $Hb\bar{b}$ form factor $F_b$ at the four-loop order. Solid and curly lines represent massless quarks and gluons, respectively. Both planar and non-planar diagrams contribute.

$$
\begin{aligned}
C_F &= (N_c^2-1)/(2N_c),\\
C_A &= N_c,\\
d_F^{abcd}d_F^{abcd}/N_F &= (18-6N_c^2+N_c^4)(N_c^2-1)/(96N_c^3),\\
d_F^{abcd}d_A^{abcd}/N_F &= (N_c^2-1)(N_c^2+6)/48.
\end{aligned}
\tag{4}
$$

We note that diagrams where the Higgs couples to a closed quark loop do not contribute. This is clear from the fact that the Yukawa coupling requires a helicity flip and all quarks are massless in our calculation. For the same reason, there are also no $d_F^{abc}d_F^{abc}$ contributions, which are present in the case of the $\gamma^* q\bar{q}$ form factor [42].

The computation of massless four-loop form factor integrals requires advanced techniques both for the reduction to master integrals but also for the computation of the latter. For the reduction it is essential to have at hand an efficient program. For our calculation we use REDUZE 2 [43] together with the code FINRED employing finite field arithmetic and further techniques from [44–50].

For the master integrals two complementary methods are applied. The first one uses finite master integrals [51–53] in $d_0-2\epsilon$ dimensions where $d_0=4,6,\ldots$, and applies the program HYPERINT [54] in cases where the corresponding Feynman parametric representation can be rendered linearly reducible [55,56]. In this approach, the actual integration is applied to individual master integrals. The second method considers all master integrals of a given integral family at the same time. In the first step one of the massless external legs is made massive. Choosing $q_1^2\neq 0$ it is possible to define $x=q_1^2/q^2$, where $q^2$ is the virtuality of the Higgs boson. Our aim is the computation of the master integrals for $x=0$. On the other hand, for $x=1$ the vertex integrals turn into massless two-point functions, which are well studied in the literature [57,58]. It is, indeed, possible to use the powerful method of differential equations [59–64] to transport the information from $x=1$ to $x=0$. For more details on this approach we refer to Ref. [33]. All master integrals needed for this work have previously been used in the literature (see, e.g., Ref. [65]). We obtain for the bare four-loop form factor

$$
\begin{aligned}
F_b^{(4)} = {}& C_F^4\left[\frac{1}{\epsilon^8}\left(\frac{2}{3}\right)+\frac{1}{\epsilon^6}\left(-\frac{4}{3}\zeta_2+\frac{8}{3}\right)+\frac{1}{\epsilon^5}\left(-\frac{272}{9}\zeta_3+12\zeta_2+\frac{16}{3}\right)+\frac{1}{\epsilon^4}\left(-\frac{296}{15}\zeta_2^2-60\zeta_3+\frac{80}{3}\zeta_2+\frac{68}{3}\right)\right.\\
&+\frac{1}{\epsilon^3}\left(-\frac{3008}{15}\zeta_5+\frac{640}{9}\zeta_3\zeta_2-12\zeta_2^2-\frac{2336}{9}\zeta_3+\frac{340}{3}\zeta_2+52\right)+\frac{1}{\epsilon^2}\left(\frac{19360}{27}\zeta_3^2-\frac{6784}{315}\zeta_2^3-1100\zeta_5-480\zeta_3\zeta_2\right.\\
&\left.+\frac{118}{15}\zeta_2^2+\frac{668}{9}\zeta_3+506\zeta_2-\frac{254}{3}\right)+\frac{1}{\epsilon}\left(-\frac{14162}{21}\zeta_7+\frac{5792}{5}\zeta_5\zeta_2+\frac{6208}{9}\zeta_3\zeta_2^2-1180\zeta_3^2-\frac{17326}{21}\zeta_2^3-\frac{113542}{15}\zeta_5\right.\\
&\left.-\frac{21398}{9}\zeta_3\zeta_2+\frac{4867}{5}\zeta_2^2+\frac{69733}{9}\zeta_3+\frac{5159}{2}\zeta_2-\frac{12707}{6}\right)+\left(-\frac{32384}{15}\zeta_{5,3}+\frac{739328}{45}\zeta_5\zeta_3-\frac{66392}{27}\zeta_3^2\zeta_2\right.\\
&+\frac{7486576}{7875}\zeta_2^4-\frac{47217}{2}\zeta_7-\frac{31928}{5}\zeta_5\zeta_2-\frac{11092}{5}\zeta_3\zeta_2^2-\frac{284228}{27}\zeta_3^2-\frac{250138}{45}\zeta_2^3-\frac{392059}{15}\zeta_5-\frac{121270}{9}\zeta_3\zeta_2\\
&\left.\left.+\frac{28514}{3}\zeta_2^2+\frac{212006}{3}\zeta_3+\frac{53859}{4}\zeta_2-\frac{71295}{4}\right)\right]+C_F^3C_A\left[\frac{1}{\epsilon^7}\left(-\frac{11}{3}\right)+\frac{1}{\epsilon^6}\left(2\zeta_2-\frac{67}{9}\right)+\frac{1}{\epsilon^5}\left(26\zeta_3-\frac{638}{27}\right)\right.\\
&+\frac{1}{\epsilon^4}\left(\frac{78}{5}\zeta_2^2+\frac{2018}{9}\zeta_3-\frac{209}{3}\zeta_2-\frac{5704}{81}\right)+\frac{1}{\epsilon^3}\left(182\zeta_5-96\zeta_3\zeta_2+\frac{7096}{45}\zeta_2^2+\frac{27823}{27}\zeta_3-\frac{3505}{9}\zeta_2-\frac{53285}{243}\right)\\
&+\frac{1}{\epsilon^2}\left(-854\zeta_3^2+\frac{13976}{315}\zeta_2^3+\frac{71882}{45}\zeta_5+\frac{2272}{9}\zeta_3\zeta_2+\frac{50633}{135}\zeta_2^2+\frac{279512}{81}\zeta_3-\frac{96061}{54}\zeta_2-\frac{846803}{1458}\right)\\
&+\frac{1}{\epsilon}\left(6172\zeta_7-\frac{11548}{5}\zeta_5\zeta_2-\frac{10508}{15}\zeta_3\zeta_2^2-\frac{214747}{27}\zeta_3^2+\frac{173389}{945}\zeta_2^3+\frac{1950199}{135}\zeta_5+\frac{162041}{27}\zeta_3\zeta_2+\frac{2971}{162}\zeta_2^2\right.\\
&\left.+\frac{938374}{243}\zeta_3-\frac{2756239}{324}\zeta_2+\frac{2800297}{8748}\right)+\left(\frac{20948}{15}\zeta_{5,3}-\frac{18364}{5}\zeta_5\zeta_3+\frac{3296}{9}\zeta_3^2\zeta_2+\frac{5472536}{2625}\zeta_2^4-\frac{933223}{56}\zeta_7\right.\\
&+\frac{69307}{9}\zeta_5\zeta_2-\frac{262058}{27}\zeta_3\zeta_2^2-\frac{803111}{81}\zeta_3^2+\frac{49163803}{5670}\zeta_2^3+\frac{141880529}{1620}\zeta_5+\frac{7016987}{162}\zeta_3\zeta_2-\frac{9911939}{972}\zeta_2^2\\
&\left.\left.-\frac{219806467}{2916}\zeta_3-\frac{84811717}{1944}\zeta_2+\frac{1218736471}{52488}\right)\right]+C_F^2C_A^2\left[\frac{1}{\epsilon^6}\left(\frac{4961}{648}\right)+\frac{1}{\epsilon^5}\left(-\frac{451}{54}\zeta_2+\frac{32665}{972}\right)\right.
\end{aligned}
$$

$$
+\frac{1}{\epsilon^4}\left(\frac{397}{90}\zeta_2^2-\frac{7975}{54}\zeta_3+\frac{371}{36}\zeta_2+\frac{209435}{1944}\right)+\frac{1}{\epsilon^3}\left(\frac{272}{3}\zeta_5+\frac{293}{9}\zeta_3\zeta_2-\frac{32843}{270}\zeta_2^2-\frac{242806}{243}\zeta_3+\frac{117517}{486}\zeta_2+\frac{1236571}{4374}\right)
$$

$$
+\frac{1}{\epsilon^2}\left(\frac{6065}{18}\zeta_3^2+\frac{67988}{945}\zeta_2^3-\frac{21511}{18}\zeta_5+\frac{25544}{81}\zeta_3\zeta_2-\frac{84901}{135}\zeta_2^2-\frac{3787327}{729}\zeta_3+\frac{5009207}{2916}\zeta_2+\frac{6218239}{13122}\right)
$$

$$
+\frac{1}{\epsilon}\left(-\frac{38323}{18}\zeta_7+\frac{7921}{9}\zeta_5\zeta_2+\frac{35767}{135}\zeta_3\zeta_2^2+\frac{590333}{81}\zeta_3^2-\frac{74927}{315}\zeta_2^3-\frac{6243851}{810}\zeta_5-\frac{83435}{27}\zeta_3\zeta_2-\frac{516463}{243}\zeta_2^2\right.
$$

$$
\left.-\frac{14345651}{729}\zeta_3+\frac{28502297}{2916}\zeta_2-\frac{15113323}{13122}\right)+\left(\frac{54254}{45}\zeta_{5,3}-\frac{45281}{9}\zeta_5\zeta_3+\frac{38482}{27}\zeta_3^2\zeta_2-\frac{21476059}{15750}\zeta_2^4\right.
$$

$$
-\frac{2480981}{144}\zeta_7+\frac{1053169}{270}\zeta_5\zeta_2+\frac{3609022}{405}\zeta_3\zeta_2^2+\frac{33473012}{729}\zeta_3^2-\frac{1870121}{1260}\zeta_2^3-\frac{122474347}{1944}\zeta_5-\frac{116700197}{2916}\zeta_3\zeta_2
$$

$$
\left.\left.-\frac{31578173}{14580}\zeta_2^2-\frac{1935211669}{52488}\zeta_3+\frac{338298976}{6561}\zeta_2-\frac{4866548501}{236196}\right)\right]+C_FC_A^3\left[\frac{1}{\epsilon^5}\left(-\frac{1331}{216}\right)+\frac{1}{\epsilon^4}\left(\frac{121}{12}\zeta_2-\frac{1067}{24}\right)\right.
$$

$$
+\frac{1}{\epsilon^3}\left(-\frac{121}{10}\zeta_2^2+\frac{3025}{12}\zeta_3-\frac{1927}{108}\zeta_2-\frac{39727}{216}\right)+\frac{1}{\epsilon^2}\left(\frac{1}{2}\zeta_3^2+\frac{626}{105}\zeta_2^3-\frac{13013}{36}\zeta_5-77\zeta_3\zeta_2+\frac{2893}{12}\zeta_2^2+\frac{164719}{81}\zeta_3\right.
$$

$$
\left.-\frac{14963}{36}\zeta_2-\frac{4881089}{11664}\right)+\frac{1}{\epsilon}\left(\frac{45511}{48}\zeta_7-\frac{206}{3}\zeta_5\zeta_2+\frac{1033}{30}\zeta_3\zeta_2^2-\frac{52547}{36}\zeta_3^2-\frac{44204}{135}\zeta_2^3+\frac{136685}{108}\zeta_5-\frac{1936}{9}\zeta_3\zeta_2\right.
$$

$$
\left.+\frac{176134}{135}\zeta_2^2+\frac{573931}{54}\zeta_3-\frac{1980005}{648}\zeta_2+\frac{6220123}{5832}\right)+\left(-\frac{14161}{30}\zeta_{5,3}+\frac{21577}{6}\zeta_5\zeta_3-\frac{1963}{3}\zeta_3^2\zeta_2+\frac{10233079}{15750}\zeta_2^4\right.
$$

$$
+\frac{79877}{48}\zeta_7-\frac{7744}{9}\zeta_5\zeta_2-\frac{71776}{45}\zeta_3\zeta_2^2-\frac{2569009}{108}\zeta_3^2-\frac{8387389}{11340}\zeta_2^3+\frac{56929927}{3240}\zeta_5+\frac{2563075}{324}\zeta_3\zeta_2+\frac{802607}{180}\zeta_2^2
$$

$$
\left.\left.+\frac{6792233}{162}\zeta_3-\frac{208858685}{11664}\zeta_2+\frac{3047508671}{139968}\right)\right]+\frac{d_F^{abcd}d_A^{abcd}}{N_F}\left[\frac{1}{\epsilon^2}\left(12\zeta_3^2+\frac{248}{35}\zeta_2^3-\frac{110}{3}\zeta_5-\frac{4}{3}\zeta_3+4\zeta_2\right)\right.
$$

$$
+\frac{1}{\epsilon}\left(-\frac{871}{2}\zeta_7-128\zeta_5\zeta_2+\frac{92}{5}\zeta_3\zeta_2^2+\frac{418}{3}\zeta_3^2-\frac{3476}{315}\zeta_2^3+\frac{230}{9}\zeta_5+224\zeta_3\zeta_2-\frac{28}{15}\zeta_2^2+\frac{1516}{9}\zeta_3+\frac{272}{3}\zeta_2-32\right)
$$

$$
+\left(260\zeta_{5,3}-5092\zeta_5\zeta_3-16\zeta_3^2\zeta_2-\frac{496766}{525}\zeta_2^4-1228\zeta_7-\frac{12808}{3}\zeta_5\zeta_2+\frac{14216}{15}\zeta_3\zeta_2^2+\frac{72674}{9}\zeta_3^2+\frac{768632}{945}\zeta_2^3\right.
$$

$$
\left.\left.-\frac{65546}{27}\zeta_5+\frac{2516}{3}\zeta_3\zeta_2+\frac{8692}{45}\zeta_2^2+\frac{112346}{27}\zeta_3+\frac{8194}{9}\zeta_2-\frac{1588}{3}\right)\right]+n_fC_F^3\left[\frac{1}{\epsilon^7}\left(\frac{2}{3}\right)+\frac{1}{\epsilon^6}\left(\frac{10}{9}\right)+\frac{1}{\epsilon^5}\left(\frac{116}{27}\right)\right.
$$

$$
+\frac{1}{\epsilon^4}\left(-\frac{92}{3}\zeta_3+\frac{38}{3}\zeta_2+\frac{898}{81}\right)+\frac{1}{\epsilon^3}\left(-\frac{844}{45}\zeta_2^2-\frac{1318}{9}\zeta_3+\frac{178}{3}\zeta_2+\frac{67063}{1944}\right)+\frac{1}{\epsilon^2}\left(-\frac{4234}{45}\zeta_5+\frac{736}{9}\zeta_3\zeta_2\right.
$$

$$
\left.-\frac{5318}{135}\zeta_2^2-\frac{38501}{54}\zeta_3+\frac{2207}{9}\zeta_2+\frac{586997}{5832}\right)+\frac{1}{\epsilon}\left(\frac{36410}{27}\zeta_3^2+\frac{169268}{945}\zeta_2^3-\frac{55498}{27}\zeta_5-\frac{6784}{27}\zeta_3\zeta_2-\frac{97709}{810}\zeta_2^2\right.
$$

$$
\left.-\frac{199787}{81}\zeta_3+\frac{114713}{108}\zeta_2+\frac{5808187}{69984}\right)+\left(\frac{1153615}{126}\zeta_7+\frac{6316}{9}\zeta_5\zeta_2+\frac{229468}{135}\zeta_3\zeta_2^2+\frac{124198}{81}\zeta_3^2-\frac{342292}{567}\zeta_2^3\right.
$$

$$
\left.\left.-\frac{13555259}{810}\zeta_5-\frac{223877}{81}\zeta_3\zeta_2+\frac{222727}{1215}\zeta_2^2-\frac{639475}{972}\zeta_3+\frac{405517}{81}\zeta_2-\frac{252681119}{104976}\right)\right]
$$

$$
+n_fC_F^2C_A\left[\frac{1}{\epsilon^6}\left(-\frac{451}{162}\right)+\frac{1}{\epsilon^5}\left(\frac{41}{27}\zeta_2-\frac{2681}{243}\right)+\frac{1}{\epsilon^4}\left(\frac{629}{27}\zeta_3-\frac{598}{81}\zeta_2-\frac{17945}{486}\right)+\frac{1}{\epsilon^3}\left(\frac{2737}{135}\zeta_2^2+\frac{56570}{243}\zeta_3\right.\right.
$$

$$
\left.-\frac{503}{6}\zeta_2-\frac{1887077}{17496}\right)+\frac{1}{\epsilon^2}\left(\frac{632}{3}\zeta_5-\frac{7328}{81}\zeta_3\zeta_2+\frac{50002}{405}\zeta_2^2+\frac{1051067}{729}\zeta_3-\frac{1532465}{2916}\zeta_2-\frac{28195033}{104976}\right)
$$

$$
+\frac{1}{\epsilon}\left(-\frac{81152}{81}\zeta_3^2+\frac{8954}{315}\zeta_2^3+\frac{607772}{405}\zeta_5+\frac{27844}{243}\zeta_3\zeta_2+\frac{188048}{405}\zeta_2^2+\frac{20440703}{2916}\zeta_3-\frac{46910953}{17496}\zeta_2-\frac{11426783}{23328}\right)
$$

$$
+\left(\frac{5669}{4}\zeta_7-\frac{249194}{135}\zeta_5\zeta_2-\frac{417244}{405}\zeta_3\zeta_2^2-\frac{8430847}{729}\zeta_3^2-\frac{41398}{45}\zeta_2^3+\frac{46976113}{2430}\zeta_5+\frac{132347}{27}\zeta_3\zeta_2+\frac{9178327}{7290}\zeta_2^2\right.
$$

$$
\begin{aligned}
&+\frac{1524037079}{52488}\zeta_3-\frac{447302531}{34992}\zeta_2+\frac{635981455}{3779136}\bigg)\bigg]+n_fC_FC_A^2\bigg[\frac{1}{\epsilon^5}\left(\frac{121}{36}\right)+\frac{1}{\epsilon^4}\left(-\frac{11}{3}\zeta_2+\frac{2435}{108}\right)\\
&+\frac{1}{\epsilon^3}\left(\frac{11}{5}\zeta_2^2-\frac{242}{3}\zeta_3+\frac{173}{9}\zeta_2+\frac{121619}{1296}\right)+\frac{1}{\epsilon^2}\left(\frac{1093}{18}\zeta_5+10\zeta_3\zeta_2-\frac{1313}{15}\zeta_2^2-\frac{19375}{27}\zeta_3+\frac{11839}{54}\zeta_2+\frac{2078443}{7776}\right)\\
&+\frac{1}{\epsilon}\left(\frac{2815}{18}\zeta_3^2+\frac{7493}{135}\zeta_2^3-\frac{20639}{27}\zeta_5+\frac{2540}{9}\zeta_3\zeta_2-\frac{16729}{45}\zeta_2^2-\frac{679399}{162}\zeta_3+\frac{872417}{648}\zeta_2+\frac{7711783}{46656}\right)\\
&+\bigg(\frac{6943}{24}\zeta_7+\frac{2755}{9}\zeta_5\zeta_2+\frac{1912}{45}\zeta_3\zeta_2^2+\frac{182662}{27}\zeta_3^2+\frac{1798639}{11340}\zeta_2^3-\frac{29781037}{3240}\zeta_5-\frac{115961}{108}\zeta_3\zeta_2-\frac{728249}{540}\zeta_2^2\\
&-\frac{40929727}{1944}\zeta_3+\frac{27793927}{3888}\zeta_2-\frac{1377145789}{279936}\bigg)\bigg]+n_f\frac{d_F^{abcd}d_F^{abcd}}{N_F}\bigg[\frac{1}{\epsilon^2}\left(\frac{40}{3}\zeta_5+\frac{8}{3}\zeta_3-8\zeta_2\right)\\
&+\frac{1}{\epsilon}\left(-\frac{152}{3}\zeta_3^2-\frac{1184}{315}\zeta_2^3+\frac{2720}{9}\zeta_5-16\zeta_3\zeta_2+\frac{40}{3}\zeta_2^2-\frac{416}{9}\zeta_3-\frac{568}{3}\zeta_2+64\right)\\
&+\bigg(-1240\zeta_7+\frac{992}{3}\zeta_5\zeta_2-\frac{3952}{15}\zeta_3\zeta_2^2-\frac{4504}{9}\zeta_3^2+\frac{215876}{945}\zeta_2^3+\frac{101938}{27}\zeta_5+\frac{572}{3}\zeta_3\zeta_2-\frac{8}{45}\zeta_2^2-\frac{18202}{27}\zeta_3\\
&-\frac{18254}{9}\zeta_2+\frac{3488}{3}\bigg)\bigg]+n_f^2C_F^2\bigg[\frac{1}{\epsilon^6}\left(\frac{41}{162}\right)+\frac{1}{\epsilon^5}\left(\frac{205}{243}\right)+\frac{1}{\epsilon^4}\left(\frac{73}{81}\zeta_2+\frac{497}{162}\right)+\frac{1}{\epsilon^3}\left(-\frac{2620}{243}\zeta_3+\frac{1702}{243}\zeta_2+\frac{86477}{8748}\right)\\
&+\frac{1}{\epsilon^2}\left(-\frac{1072}{405}\zeta_2^2-\frac{58276}{729}\zeta_3+\frac{3091}{81}\zeta_2+\frac{209642}{6561}\right)+\frac{1}{\epsilon}\bigg(\frac{8948}{405}\zeta_5+\frac{7808}{243}\zeta_3\zeta_2-\frac{11692}{1215}\zeta_2^2-\frac{123817}{243}\zeta_3\\
&+\frac{752095}{4374}\zeta_2+\frac{11881193}{104976}\bigg)+\bigg(\frac{689582}{729}\zeta_3^2+\frac{191252}{945}\zeta_2^3-\frac{217004}{243}\zeta_5+\frac{60584}{729}\zeta_3\zeta_2-\frac{41431}{405}\zeta_2^2-\frac{42764887}{13122}\zeta_3\\
&+\frac{9851863}{13122}\zeta_2+\frac{436438747}{944784}\bigg)\bigg]+n_f^2C_FC_A\bigg[\frac{1}{\epsilon^5}\left(-\frac{11}{18}\right)+\frac{1}{\epsilon^4}\left(\frac{1}{3}\zeta_2-\frac{197}{54}\right)+\frac{1}{\epsilon^3}\left(\frac{19}{3}\zeta_3-5\zeta_2-\frac{19819}{1296}\right)\\
&+\frac{1}{\epsilon^2}\left(\frac{39}{5}\zeta_2^2+\frac{1846}{27}\zeta_3-\frac{982}{27}\zeta_2-\frac{417697}{7776}\right)+\frac{1}{\epsilon}\left(\frac{784}{9}\zeta_5-\frac{412}{9}\zeta_3\zeta_2+\frac{502}{45}\zeta_2^2+\frac{35089}{81}\zeta_3-\frac{121495}{648}\zeta_2-\frac{7185425}{46656}\right)\\
&+\left(-\frac{1714}{3}\zeta_3^2-\frac{2836}{315}\zeta_2^3+\frac{144946}{135}\zeta_5+\frac{28}{3}\zeta_3\zeta_2+\frac{4258}{135}\zeta_2^2+\frac{1209401}{486}\zeta_3-\frac{1168375}{1296}\zeta_2-\frac{73152481}{279936}\right)\bigg]\\
&+n_f^3C_F\bigg[\frac{1}{\epsilon^5}\left(\frac{1}{27}\right)+\frac{1}{\epsilon^4}\left(\frac{5}{27}\right)+\frac{1}{\epsilon^3}\left(\frac{10}{27}\zeta_2+\frac{65}{81}\right)+\frac{1}{\epsilon^2}\left(-\frac{82}{81}\zeta_3+\frac{50}{27}\zeta_2+\frac{2537}{729}\right)\\
&+\frac{1}{\epsilon}\left(\frac{302}{135}\zeta_2^2-\frac{410}{81}\zeta_3+\frac{650}{81}\zeta_2+\frac{11408}{729}\right)+\left(-\frac{2194}{135}\zeta_5-\frac{820}{81}\zeta_3\zeta_2+\frac{302}{27}\zeta_2^2-\frac{5330}{243}\zeta_3+\frac{25370}{729}\zeta_2+\frac{159908}{2187}\right)\bigg]\\
&+\mathcal{O}(\epsilon^1).
\end{aligned}
\tag{5}
$$

Our result is expressed in terms of regular zeta values $\zeta_2$, $\zeta_3$, $\zeta_5$, $\zeta_7$ and one multiple zeta value

$$\zeta_{5,3}=\sum_{m=1}^{\infty}\sum_{n=1}^{m-1}\frac{1}{m^5n^3}\approx 0.0377076729848. \tag{6}$$

As expected for a generic four-loop form factor in QCD, the leading pole is $1/\epsilon^8$ and the finite part has transcendental weight up to 8.

We have performed the following checks on our result in Eq. (5) for the bare four-loop form factor $F_b^{(4)}$. First, we have recalculated the known $n_f^2$ and $n_f^3$ contributions and found agreement with the results of Ref. [8]; all other terms are new. For the leading color contribution we have performed two independent calculations and verified that the results agree. Furthermore, we have checked that all poles $1/\epsilon^8, \ldots, 1/\epsilon$ agree with predictions derived from known anomalous dimensions through to four-loop order and lower-loop contributions through to transcendental weight 8. This is a strong check of our result and a confirmation of the literature expression for the quark collinear anomalous dimension. Details for this derivation will be given in the sections below. For the sake of completeness, we have also recalculated the lower-loop bare form factors $F_b^{(1)}$, $F_b^{(2)}$, $F_b^{(3)}$ through to weight 8 and found full agreement with the results of Ref. [8]. We also extracted the maximal transcendental weight 8 part and find that it coincides with that of the $\gamma^* q\bar{q}$ form factor [42,65] (and, after modifying the Casimir operators such that quarks and gluons are in the adjoint color representation, also with that of the $Hgg$ form factor [42,65]).

## III. UV RENORMALIZATION FOR $Hb\bar{b}$, $\gamma^* q\bar{q}$, AND $Hgg$ FORM FACTORS

In this section, we discuss the UV renormalization of different form factors, focusing first on the $Hb\bar{b}$ form factor. We perform UV renormalization in the $\overline{\mathrm{MS}}$ scheme and replace the bare couplings $a_0$ and $y_0$ by the renormalized couplings $a$ and $y$ with

$$S_\epsilon \mu_0^{2\epsilon} a_0 = Z_a \mu^{2\epsilon} a, \tag{7}$$

$$y_0 = Z_m y. \tag{8}$$

With the $\beta$ function and the quark anomalous dimension $\gamma^m$

$$\beta(a) = -a \frac{\mathrm{d}\ln Z_a}{\mathrm{d}\ln \mu^2} = -a^2 \sum_{n=0}^{\infty} a^n \beta_n, \tag{9}$$

$$\gamma^m(a) = -\frac{\mathrm{d}\ln Z_m}{\mathrm{d}\ln \mu^2} = -a \sum_{n=0}^{\infty} a^n \gamma_n^m, \tag{10}$$

one has from (7) for the renormalized coupling $\mathrm{d}a/\mathrm{d}\ln\mu^2 = \beta - a\epsilon$ and thus

$$\frac{\mathrm{d}\ln Z_a}{\mathrm{d}a} = -\frac{\beta}{a(\beta - a\epsilon)}, \tag{11}$$

$$\frac{\mathrm{d}\ln Z_m}{\mathrm{d}a} = -\frac{\gamma^m}{\beta - a\epsilon}. \tag{12}$$

Solving these differential equations perturbatively results in

$$Z_a = 1 + a\left(-\frac{\beta_0}{\epsilon}\right) + a^2\left(\frac{\beta_0^2}{\epsilon^2} - \frac{\beta_1}{2\epsilon}\right) + a^3\left(\frac{7\beta_0\beta_1}{6\epsilon^2} - \frac{\beta_0^3}{\epsilon^3} - \frac{\beta_2}{3\epsilon}\right) + a^4\left(\frac{\beta_0^4}{\epsilon^4} - \frac{23\beta_0^2\beta_1}{12\epsilon^3} + \frac{9\beta_1^2 + 20\beta_0\beta_2}{24\epsilon^2} - \frac{\beta_3}{4\epsilon}\right) + \mathcal{O}(a^5), \tag{13}$$

$$\begin{aligned} Z_m = {}& 1 + a\left(-\frac{\gamma_0^m}{\epsilon}\right) + a^2\left(\frac{\gamma_0^m(\beta_0 + \gamma_0^m)}{2\epsilon^2} - \frac{\gamma_1^m}{2\epsilon}\right) + a^3\left(-\frac{\gamma_0^m(\beta_0 + \gamma_0^m)(2\beta_0 + \gamma_0^m)}{6\epsilon^3} + \frac{2\beta_1\gamma_0^m + 2\beta_0\gamma_1^m + 3\gamma_0^m\gamma_1^m}{6\epsilon^2} + \frac{\gamma_2^m}{3\epsilon}\right) \\ & + a^4\left(\frac{\gamma_0^m(\beta_0 + \gamma_0^m)(2\beta_0 + \gamma_0^m)(3\beta_0 + \gamma_0^m)}{24\epsilon^4} + \frac{-6\beta_0\beta_1\gamma_0^m - 4\beta_1(\gamma_0^m)^2 - 3\beta_0^2\gamma_1^m - 7\beta_0\gamma_0^m\gamma_1^m - 3(\gamma_0^m)^2\gamma_1^m}{12\epsilon^3}\right. \\ & \left. + \frac{6\beta_2\gamma_0^m + 6\beta_1\gamma_1^m + 3(\gamma_1^m)^2 + 6\beta_0\gamma_2^m + 8\gamma_0^m\gamma_2^m}{24\epsilon^2} - \frac{\gamma_3^m}{4\epsilon}\right) + \mathcal{O}(a^5). \end{aligned} \tag{14}$$

The coefficients of the $\beta$ function read [66,67]

$$\beta_0 = C_A\left(\frac{11}{3}\right) + n_f\left(-\frac{2}{3}\right), \tag{15}$$

$$\beta_1 = C_A^2\left(\frac{34}{3}\right) + n_f C_A\left(-\frac{10}{3}\right) + n_f C_F(-2), \tag{16}$$

$$\beta_2 = C_A^3\left(\frac{2857}{54}\right) + n_f C_A^2\left(-\frac{1415}{54}\right) + n_f C_A C_F\left(-\frac{205}{18}\right) + n_f C_F^2(1) + n_f^2 C_A\left(\frac{79}{54}\right) + n_f^2 C_F\left(\frac{11}{9}\right), \tag{17}$$

$$\begin{aligned} \beta_3 = {}& C_A^4\left(-\frac{44}{9}\zeta_3 + \frac{150653}{486}\right) + \frac{d_A^{abcd}d_A^{abcd}}{N_A}\left(\frac{704}{3}\zeta_3 - \frac{80}{9}\right) + n_f C_A^3\left(\frac{68}{3}\zeta_3 - \frac{39143}{162}\right) + n_f C_A^2 C_F\left(-\frac{328}{9}\zeta_3 + \frac{7073}{486}\right) \\ & + n_f C_A C_F^2\left(\frac{176}{9}\zeta_3 - \frac{2102}{27}\right) + n_f C_F^3(23) + n_f\frac{d_A^{abcd}d_F^{abcd}}{N_A}\left(-\frac{1664}{3}\zeta_3 + \frac{512}{9}\right) + n_f^2 C_A^2\left(\frac{56}{9}\zeta_3 + \frac{3965}{162}\right) \\ & + n_f^2 C_A C_F\left(\frac{112}{9}\zeta_3 + \frac{4288}{243}\right) + n_f^2 C_F^2\left(-\frac{176}{9}\zeta_3 + \frac{338}{27}\right) + n_f^2\frac{d_F^{abcd}d_F^{abcd}}{N_A}\left(\frac{512}{3}\zeta_3 - \frac{704}{9}\right) + n_f^3 C_A\left(\frac{53}{243}\right) \\ & + n_f^3 C_F\left(\frac{154}{243}\right), \end{aligned} \tag{18}$$

and the coefficients of the quark mass anomalous dimension are given by [68,69]

$$\gamma_0^m = C_F(3), \tag{19}$$

$$\gamma_1^m = C_F C_A\left(\frac{97}{6}\right) + C_F^2\left(\frac{3}{2}\right) + n_f C_F\left(-\frac{10}{6}\right), \tag{20}$$

$$\gamma_2^m = C_F^3\left(\frac{129}{2}\right) + C_F^2 C_A\left(-\frac{129}{4}\right) + C_F C_A^2\left(\frac{11413}{108}\right) + n_f C_F^2(24\zeta_3 - 23) + n_f C_F C_A\left(-24\zeta_3 - \frac{278}{27}\right) + n_f^2 C_F\left(-\frac{35}{27}\right), \tag{21}$$

$$\begin{aligned}\gamma_3^m = {} & C_F^4\left(-336\zeta_3 - \frac{1261}{8}\right) + C_F^3 C_A\left(316\zeta_3 + \frac{15349}{12}\right) + C_F^2 C_A^2\left(440\zeta_5 - 152\zeta_3 - \frac{34045}{36}\right)\\ & + C_F C_A^3\left(-440\zeta_5 + \frac{1418}{9}\zeta_3 + \frac{70055}{72}\right) + \frac{d_F^{abcd}d_A^{abcd}}{N_F}(240\zeta_3 - 32) + n_f C_F^3\left(-240\zeta_5 + 276\zeta_3 - \frac{140}{3}\right)\\ & + n_f C_F^2 C_A\left(-132\zeta_4 + 40\zeta_5 + 184\zeta_3 - \frac{8819}{54}\right) + n_f C_F C_A^2\left(132\zeta_4 + 200\zeta_5 - \frac{1342}{3}\zeta_3 - \frac{65459}{324}\right)\\ & + n_f \frac{d_F^{abcd}d_F^{abcd}}{N_F}(-480\zeta_3 + 64) + n_f^2 C_F^2\left(24\zeta_4 - 40\zeta_3 + \frac{76}{27}\right) + n_f^2 C_F C_A\left(-24\zeta_4 + 40\zeta_3 + \frac{671}{162}\right)\\ & + n_f^3 C_F\left(\frac{16}{9}\zeta_3 - \frac{83}{81}\right).\end{aligned} \tag{22}$$

In addition to the $Hb\bar{b}$ form factor (1), we consider also the UV renormalization of the bare form factors for the $\gamma^* q\bar{q}$ and $Hgg$ vertices

$$\mathcal{F}_q = -\frac{1}{4(1-\epsilon)q^2}\mathrm{Tr}(\not{q}_2\Gamma_q^\mu \not{q}_1\gamma_\mu), \tag{23}$$

$$\mathcal{F}_g = \frac{(q_1\cdot q_2 g_{\mu\nu} - q_{1,\mu}q_{2,\nu} - q_{1,\nu}q_{2,\mu})}{2(1-\epsilon)}\Gamma_g^{\mu\nu}. \tag{24}$$

Here, the projections are applied to the $\gamma^* q\bar{q}$ and $Hgg$ vertex functions $\Gamma_q^\mu$ and $\Gamma_g^{\mu\nu}$. The $Hgg$ interaction is taken in the infinite top-quark-mass limit, where it can be described by the bare effective Lagrangian

$$\mathcal{L}_{\mathrm{eff}} = -\frac{\lambda_0}{4} H F_a^{\mu\nu} F_{a,\mu\nu}. \tag{25}$$

The bare form factor $\mathcal{F}_g$ depends on the bare coupling $\lambda_0$, which is renormalized according to

$$\lambda_0 = Z_\lambda \lambda, \tag{26}$$

where the renormalization constant $Z_\lambda$ is given to all orders by coefficients of the QCD $\beta$-function [70],

$$\begin{aligned} Z_\lambda &= \frac{1}{1-\beta/(a\epsilon)}\\ &= 1 - a\frac{\beta_0}{\epsilon} + a^2\left(\frac{\beta_0^2}{\epsilon^2} - \frac{\beta_1}{\epsilon}\right) + a^3\left(-\frac{\beta_0^3}{\epsilon^3} + \frac{2\beta_0\beta_1}{\epsilon^2} - \frac{\beta_2}{\epsilon}\right)\\ &\quad + a^4\left(\frac{\beta_0^4}{\epsilon^4} - \frac{3\beta_0^2\beta_1}{\epsilon^3} + \frac{\beta_1^2 + 2\beta_0\beta_2}{\epsilon^2} - \frac{\beta_3}{\epsilon}\right) + \mathcal{O}(a^5). \end{aligned} \tag{27}$$

In summary, we arrive at the renormalized form factors for the $Hb\bar{b}$, $\gamma^* q\bar{q}$, and $Hgg$ vertices, respectively,

$$\mathcal{F}_b^{\mathrm{ren}} = yZ_m\left[1 + \sum_{n\geq 1}(aZ_a)^n e^{-n\epsilon L} F_b^{(n)},\right] = yF_b^{\mathrm{ren}}, \tag{28}$$

$$\mathcal{F}_q^{\mathrm{ren}} = 1 + \sum_{n\geq 1}(aZ_a)^n e^{-n\epsilon L} F_q^{(n)} = F_q^{\mathrm{ren}}, \tag{29}$$

$$\mathcal{F}_g^{\mathrm{ren}} = \lambda Z_\lambda\left[1 + \sum_{n\geq 1}(aZ_a)^n e^{-n\epsilon L} F_g^{(n)}\right] = \lambda F_g^{\mathrm{ren}}, \tag{30}$$

where

$$L \equiv \ln\left(\frac{-q^2 - i0}{\mu^2}\right) \tag{31}$$

contains the dependence on the renormalization scale.

## IV. IR SUBTRACTION FOR $Hb\bar{b}$, $\gamma^* q\bar{q}$, AND $Hgg$ FORM FACTORS

We begin by considering a general UV renormalized scattering amplitude $\mathcal{M}^{\text{ren}}$ with IR poles in $\epsilon$. These divergences shall be absorbed by introducing a quantity $\mathbf{Z}$ such that

$$\mathcal{M}^{\text{fin}} = \mathbf{Z}^{-1}\mathcal{M}^{\text{ren}}, \tag{32}$$

where $\mathcal{M}^{\text{fin}}$ is finite for $\epsilon \to 0$. For strongly interacting external states, $\mathcal{M}^{\text{ren}}$ and $\mathcal{M}^{\text{fin}}$ are vectors in color space and $\mathbf{Z}$ is a matrix. Interestingly, the matrix $\mathbf{Z}$ exhibits universal, process-independent features (see [71] for a recent review). Defining the anomalous dimension matrix $\mathbf{\Gamma}$ via

$$\mathbf{\Gamma}(\mu, a) = -\mathbf{Z}^{-1}\frac{\mathrm{d}\mathbf{Z}}{\mathrm{d}\ln\mu} \tag{33}$$

the matrix $\mathbf{Z}$ can be expressed as [32]

$$\ln\mathbf{Z} = -\frac{1}{2}\int_0^a \frac{\mathrm{d}a'}{\beta(a') - \epsilon a'}\left(\mathbf{\Gamma}(\mu, a') - \frac{1}{2}\int_0^{a'}\frac{\mathrm{d}a''\Gamma'(a'')}{\beta(a'') - \epsilon a''}\right). \tag{34}$$

Expansion in $a$ according to Eq. (9),

$$\mathbf{\Gamma}(\mu, a) = \sum_{n=1}^{\infty} a^n \mathbf{\Gamma}_n(\mu), \tag{35}$$

$$\Gamma'(a) = \frac{\mathrm{d}\mathbf{\Gamma}(\mu, a)}{\mathrm{d}\ln(\mu)} = \sum_{n=1}^{\infty} a^n \Gamma'_n, \tag{36}$$

and integration gives [72]

$$\begin{aligned}\ln\mathbf{Z} = {}& a\left(\frac{\Gamma'_1}{4\epsilon^2} + \frac{\mathbf{\Gamma}_1}{2\epsilon}\right) + a^2\left(-\frac{3\beta_0\Gamma'_1}{16\epsilon^3} + \frac{\Gamma'_2 - 4\beta_0\mathbf{\Gamma}_1}{16\epsilon^2} + \frac{\mathbf{\Gamma}_2}{4\epsilon}\right) + a^3\left(\frac{11\beta_0^2\Gamma'_1}{72\epsilon^4} + \frac{12\beta_0^2\mathbf{\Gamma}_1 - 8\beta_1\Gamma'_1 - 5\beta_0\Gamma'_2}{72\epsilon^3}\right.\\ &\left. + \frac{\Gamma'_3 - 6\beta_0\mathbf{\Gamma}_2 - 6\beta_1\mathbf{\Gamma}_1}{36\epsilon^2} + \frac{\mathbf{\Gamma}_3}{6\epsilon}\right) + a^4\left(-\frac{25\beta_0^3\Gamma'_1}{192\epsilon^5} + \frac{\beta_0(13\beta_0\Gamma'_2 + 40\beta_1\Gamma'_1 - 24\beta_0^2\mathbf{\Gamma}_1)}{192\epsilon^4}\right.\\ &\left. + \frac{-7\beta_0\Gamma'_3 - 9\beta_1\Gamma'_2 + 24\beta_0^2\mathbf{\Gamma}_2 - 15\beta_2\Gamma'_1 + 48\beta_0\beta_1\mathbf{\Gamma}_1}{192\epsilon^3} + \frac{\Gamma'_4 - 8\beta_0\mathbf{\Gamma}_3 - 8\beta_1\mathbf{\Gamma}_2 - 8\beta_2\mathbf{\Gamma}_1}{64\epsilon^2} + \frac{\mathbf{\Gamma}_4}{8\epsilon}\right) + \mathcal{O}(a^5).\end{aligned} \tag{37}$$

Through to three loops, the matrices $\mathbf{\Gamma}_n$ and $\Gamma'_n$ are known [31,32,73–78] in terms of cusp and collinear anomalous dimensions, depending only on the type of external state. In particular, they contain a sum over so-called dipole contributions, each of which is generated from color correlations of two external states. Starting at three loops, also quadrupole contributions involving three or four external partons at a time appear [72,78–81] through the anomalous dimension matrix $\mathbf{Z}$. At four loops, structural information about the matrix $\mathbf{Z}$ is available [72,82–84], but its complete expression is not known yet.

For four-loop form factors with only two colored external states, there is only one dipole contribution and the structure simplifies significantly. In particular, the matrix $\mathbf{Z}$ becomes diagonal and (see [32])

$$\mathbf{Z} = Z_r, \tag{38}$$

$$\mathbf{\Gamma}_n = -\Gamma_n^r \ln\left(\frac{\mu^2}{-q^2 - i0}\right) - \gamma_n^r, \tag{39}$$

$$\Gamma'_n = -2\Gamma_n^r, \tag{40}$$

where $r = q, g$ denotes the type of external particle and

$$\Gamma^r(a) = \sum_{n=1}^{\infty} a^n \Gamma_n^r, \tag{41}$$

$$\gamma^r(a) = \sum_{n=1}^{\infty} a^n \gamma_n^r \tag{42}$$

are the cusp and collinear anomalous dimensions, respectively. The coefficients of the cusp anomalous dimension through to four-loop order are [35,36]

$$\Gamma_1^r = C_R(4), \tag{43}$$

$$\Gamma_2^r = C_R C_A\left(-8\zeta_2 + \frac{268}{9}\right) + n_f C_R\left(-\frac{40}{9}\right), \tag{44}$$

$$\begin{aligned}\Gamma_3^r = {}& C_R C_A^2\left(\frac{176}{5}\zeta_2^2 + \frac{88}{3}\zeta_3 - \frac{1072}{9}\zeta_2 + \frac{490}{3}\right)\\ & + n_f C_R C_A\left(-\frac{112}{3}\zeta_3 + \frac{160}{9}\zeta_2 - \frac{836}{27}\right)\\ & + n_f C_R C_F\left(32\zeta_3 - \frac{110}{3}\right) + n_f^2 C_R\left(-\frac{16}{27}\right),\end{aligned} \tag{45}$$

$$\Gamma_4^r = C_R C_A^3\left(-16\zeta_3^2 - \frac{20032}{105}\zeta_2^3 - \frac{3608}{9}\zeta_5 - \frac{352}{3}\zeta_3\zeta_2 + \frac{3608}{5}\zeta_2^2 + \frac{20944}{27}\zeta_3 - \frac{88400}{81}\zeta_2 + \frac{84278}{81}\right) + \frac{d_R^{abcd}d_A^{abcd}}{N_R}\left(-384\zeta_3^2 - \frac{7936}{35}\zeta_2^3 + \frac{3520}{3}\zeta_5 + \frac{128}{3}\zeta_3 - 128\zeta_2\right) + n_f C_R C_A^2\left(\frac{2096}{9}\zeta_5 + \frac{448}{3}\zeta_3\zeta_2 - \frac{352}{15}\zeta_2^2 - \frac{23104}{27}\zeta_3 + \frac{20320}{81}\zeta_2 - \frac{24137}{81}\right) + n_f C_R C_A C_F\left(160\zeta_5 - 128\zeta_3\zeta_2 - \frac{352}{5}\zeta_2^2 + \frac{3712}{9}\zeta_3 + \frac{440}{3}\zeta_2 - \frac{34066}{81}\right) + n_f C_R C_F^2\left(-320\zeta_5 + \frac{592}{3}\zeta_3 + \frac{572}{9}\right) + n_f\frac{d_R^{abcd}d_F^{abcd}}{N_R}\left(-\frac{1280}{3}\zeta_5 - \frac{256}{3}\zeta_3 + 256\zeta_2\right) + n_f^2 C_R C_A\left(-\frac{224}{15}\zeta_2^2 + \frac{2240}{27}\zeta_3 - \frac{608}{81}\zeta_2 + \frac{923}{81}\right) + n_f^2 C_R C_F\left(\frac{64}{5}\zeta_2^2 - \frac{640}{9}\zeta_3 + \frac{2392}{81}\right) + n_f^3 C_R\left(\frac{64}{27}\zeta_3 - \frac{32}{81}\right), \tag{46}$$

where $R = F$ for $r = q$ and $R = A$ for $r = g$. The collinear anomalous dimensions are known to four-loop order as well [36,37], and the coefficients read

$$\gamma_1^q = C_F(6), \tag{47}$$

$$\gamma_2^q = C_F^2(48\zeta_3 - 24\zeta_2 + 3) + C_F C_A\left(-52\zeta_3 + 22\zeta_2 + \frac{961}{27}\right) + n_f C_F\left(-4\zeta_2 - \frac{130}{27}\right), \tag{48}$$

$$\gamma_3^q = C_F^3\left(-480\zeta_5 - 64\zeta_3\zeta_2 + \frac{576}{5}\zeta_2^2 + 136\zeta_3 + 36\zeta_2 + 29\right) + C_F^2 C_A\left(240\zeta_5 + 32\zeta_3\zeta_2 - \frac{1976}{15}\zeta_2^2 + \frac{1688}{3}\zeta_3 - \frac{820}{3}\zeta_2 + \frac{151}{2}\right) + C_F C_A^2\left(272\zeta_5 + \frac{176}{3}\zeta_3\zeta_2 + \frac{332}{5}\zeta_2^2 - \frac{7052}{9}\zeta_3 + \frac{14326}{81}\zeta_2 + \frac{139345}{1458}\right) + n_f C_F^2\left(\frac{112}{3}\zeta_2^2 - \frac{512}{9}\zeta_3 + \frac{52}{3}\zeta_2 - \frac{2953}{27}\right) + n_f C_F C_A\left(-\frac{88}{5}\zeta_2^2 + \frac{1928}{27}\zeta_3 - \frac{5188}{81}\zeta_2 + \frac{17318}{729}\right) + n_f^2 C_F\left(\frac{16}{27}\zeta_3 + \frac{40}{9}\zeta_2 - \frac{4834}{729}\right), \tag{49}$$

$$\gamma_4^q = C_F^4\left(11760\zeta_7 - 768\zeta_5\zeta_2 + \frac{256}{5}\zeta_3\zeta_2^2 - 2304\zeta_3^2 - \frac{33776}{35}\zeta_2^3 - 5040\zeta_5 - 240\zeta_3\zeta_2 - \frac{1368}{5}\zeta_2^2 + 4008\zeta_3 - 900\zeta_2 + \frac{4873}{12}\right) + C_F^3 C_A\left(-21840\zeta_7 + 4128\zeta_5\zeta_2 + \frac{512}{5}\zeta_3\zeta_2^2 + 6440\zeta_3^2 + \frac{634376}{315}\zeta_2^3 - 1952\zeta_5 - \frac{3976}{3}\zeta_3\zeta_2 + \frac{8668}{5}\zeta_2^2 - 6520\zeta_3 + 2334\zeta_2 - \frac{2085}{2}\right) + C_F^2 C_A^2\left(17220\zeta_7 - 4208\zeta_5\zeta_2 - \frac{128}{5}\zeta_3\zeta_2^2 - \frac{14204}{3}\zeta_3^2 - \frac{43976}{35}\zeta_2^3 + \frac{10708}{9}\zeta_5 + \frac{4192}{9}\zeta_3\zeta_2 - \frac{48680}{27}\zeta_2^2 + \frac{259324}{27}\zeta_3 - \frac{93542}{27}\zeta_2 + \frac{29639}{18}\right) + C_F C_A^3\left(-\frac{45511}{6}\zeta_7 + \frac{1648}{3}\zeta_5\zeta_2 - \frac{4132}{15}\zeta_3\zeta_2^2 + \frac{5126}{9}\zeta_3^2 - \frac{77152}{315}\zeta_2^3 + \frac{175166}{27}\zeta_5 + \frac{15400}{9}\zeta_3\zeta_2 + \frac{186742}{135}\zeta_2^2 - \frac{1751224}{243}\zeta_3 + \frac{1062149}{729}\zeta_2 + \frac{7179083}{26244}\right) + \frac{d_F^{abcd}d_A^{abcd}}{N_F}\left(3484\zeta_7 + 1024\zeta_5\zeta_2 - \frac{736}{5}\zeta_3\zeta_2^2 - \frac{3344}{3}\zeta_3^2 + \frac{27808}{315}\zeta_2^3 - \frac{1840}{9}\zeta_5 - 1792\zeta_3\zeta_2 + \frac{224}{15}\zeta_2^2 - \frac{7808}{9}\zeta_3 - \frac{2176}{3}\zeta_2 + 192\right) + n_f C_F^3\left(368\zeta_3^2 - \frac{117344}{315}\zeta_2^3 + \frac{3872}{3}\zeta_5 - \frac{512}{3}\zeta_3\zeta_2 - \frac{668}{5}\zeta_2^2 - \frac{1120}{9}\zeta_3 + 322\zeta_2 + \frac{27949}{108}\right) + n_f C_F^2 C_A\left(-\frac{3400}{3}\zeta_3^2 + \frac{5744}{35}\zeta_2^3 - \frac{4472}{3}\zeta_5 + \frac{3904}{9}\zeta_3\zeta_2 + \frac{105488}{135}\zeta_2^2 - \frac{23518}{81}\zeta_3 + \frac{673}{27}\zeta_2 - \frac{1092511}{972}\right) + n_f C_F C_A^2\left(\frac{6916}{9}\zeta_3^2 + \frac{24184}{315}\zeta_2^3 + \frac{6088}{27}\zeta_5 - \frac{3584}{9}\zeta_3\zeta_2 - \frac{17164}{45}\zeta_2^2 + \frac{140632}{243}\zeta_3 - \frac{445117}{729}\zeta_2 + \frac{326863}{1944}\right) + n_f\frac{d_F^{abcd}d_F^{abcd}}{N_F}\left(\frac{1216}{3}\zeta_3^2 + \frac{9472}{315}\zeta_2^3 - \frac{21760}{9}\zeta_5 + 128\zeta_3\zeta_2 - \frac{320}{3}\zeta_2^2 - \frac{5312}{9}\zeta_3 + \frac{4544}{3}\zeta_2 - 384\right)$$

$$+n_f^2C_F^2\left(\frac{1040}{9}\zeta_5-\frac{224}{9}\zeta_3\zeta_2-\frac{8032}{135}\zeta_2^2-\frac{4232}{81}\zeta_3+\frac{1972}{27}\zeta_2+\frac{9965}{486}\right)+n_f^2C_FC_A\left(-\frac{1184}{9}\zeta_5+\frac{256}{9}\zeta_3\zeta_2+\frac{152}{15}\zeta_2^2+\frac{14872}{243}\zeta_3+\frac{41579}{729}\zeta_2-\frac{97189}{17496}\right)+n_f^3C_F\left(\frac{128}{135}\zeta_2^2+\frac{1424}{243}\zeta_3+\frac{16}{27}\zeta_2-\frac{37382}{6561}\right) \tag{50}$$

for the quark and

$$\gamma_1^g=C_A\left(\frac{22}{3}\right)+n_f\left(-\frac{4}{3}\right), \tag{51}$$

$$\gamma_2^g=C_A^2\left(-4\zeta_3-\frac{22}{3}\zeta_2+\frac{1384}{27}\right)+n_fC_A\left(\frac{4}{3}\zeta_2-\frac{256}{27}\right)+n_fC_F(-4), \tag{52}$$

$$\gamma_3^g=C_A^3\left(32\zeta_5+\frac{80}{3}\zeta_3\zeta_2+\frac{1276}{15}\zeta_2^2-\frac{244}{3}\zeta_3-\frac{12218}{81}\zeta_2+\frac{194372}{729}\right)+n_fC_A^2\left(-\frac{328}{15}\zeta_2^2-\frac{712}{27}\zeta_3+\frac{2396}{81}\zeta_2-\frac{30715}{729}\right)+n_fC_AC_F\left(\frac{32}{5}\zeta_2^2+\frac{304}{9}\zeta_3+4\zeta_2-\frac{2434}{27}\right)+n_fC_F^2(2)+n_f^2C_A\left(\frac{112}{27}\zeta_3-\frac{40}{27}\zeta_2+\frac{269}{729}\right)+n_f^2C_F\left(\frac{22}{9}\right), \tag{53}$$

$$\begin{aligned}\gamma_4^g=&C_A^4\left(-\frac{2671}{6}\zeta_7-\frac{896}{3}\zeta_5\zeta_2-\frac{2212}{15}\zeta_3\zeta_2^2-\frac{286}{9}\zeta_3^2-\frac{674696}{945}\zeta_2^3+\frac{19232}{27}\zeta_5+\frac{1588}{3}\zeta_3\zeta_2+\frac{249448}{135}\zeta_2^2+\frac{36380}{243}\zeta_3\right.\\&\left.-\frac{1051411}{729}\zeta_2+\frac{10672040}{6561}\right)+\frac{d_{abcd}^Ad_{abcd}^A}{N_A}\left(3484\zeta_7+1024\zeta_5\zeta_2-\frac{736}{5}\zeta_3\zeta_2^2-\frac{3344}{3}\zeta_3^2+\frac{39776}{315}\zeta_2^3+\frac{2720}{9}\zeta_5\right.\\&\left.-2336\zeta_3\zeta_2-\frac{1808}{15}\zeta_2^2-\frac{12512}{9}\zeta_3+64\zeta_2+\frac{128}{9}\right)+n_fC_A^3\left(-\frac{596}{9}\zeta_3^2+\frac{148976}{945}\zeta_2^3+\frac{16066}{27}\zeta_5+148\zeta_3\zeta_2\right.\\&\left.-\frac{69502}{135}\zeta_2^2-\frac{260822}{243}\zeta_3+\frac{155273}{729}\zeta_2-\frac{421325}{1944}\right)+n_fC_A^2C_F\left(152\zeta_3^2+\frac{5632}{315}\zeta_2^3+\frac{8}{9}\zeta_5-176\zeta_3\zeta_2-\frac{1196}{45}\zeta_2^2\right.\\&\left.+\frac{29606}{81}\zeta_3+\frac{3023}{9}\zeta_2-\frac{903983}{972}\right)+n_fC_AC_F^2\left(-80\zeta_3^2-\frac{320}{7}\zeta_2^3-\frac{1600}{3}\zeta_5+\frac{148}{5}\zeta_2^2+\frac{1592}{3}\zeta_3-2\zeta_2+\frac{685}{12}\right)\\&+n_fC_F^3(46)+n_f\frac{d_{abcd}^Ad_{abcd}^F}{N_A}\left(\frac{1216}{3}\zeta_3^2-\frac{14464}{315}\zeta_2^3-\frac{30880}{9}\zeta_5+1216\zeta_3\zeta_2+\frac{2464}{15}\zeta_2^2+\frac{2560}{9}\zeta_3-64\zeta_2+\frac{448}{9}\right)\\&+n_f^2C_A^2\left(-\frac{1024}{9}\zeta_5-32\zeta_3\zeta_2+\frac{3128}{135}\zeta_2^2+\frac{37354}{243}\zeta_3-\frac{13483}{729}\zeta_2+\frac{611939}{17496}\right)\\&+n_f^2C_AC_F\left(\frac{304}{9}\zeta_5+\frac{32}{3}\zeta_3\zeta_2+\frac{128}{45}\zeta_2^2-\frac{1688}{81}\zeta_3-\frac{172}{9}\zeta_2+\frac{1199}{18}\right)+n_f^2C_F^2\left(-\frac{352}{9}\zeta_3+\frac{676}{27}\right)\\&+n_f^2\frac{d_{abcd}^Fd_{abcd}^F}{N_A}\left(\frac{1024}{3}\zeta_3-\frac{1408}{9}\right)+n_f^3C_A\left(\frac{256}{135}\zeta_2^2-\frac{400}{243}\zeta_3-\frac{16}{81}\zeta_2-\frac{15890}{6561}\right)+n_f^3C_F\left(\frac{308}{243}\right)\end{aligned} \tag{54}$$

for the gluon. We note that the exact conventions used above differ slightly from [32], and our notation for the cusp and collinear anomalous dimensions coincide with that of Refs. [36,37]. In particular, the quantity $\gamma_i^q$ used here is $-2$ times the quantity denoted by $\gamma_{i-1}^q$ in Ref. [32].

With the above, the finite remainders for our form factors are obtained as

$$F_b^{\rm fin}=Z_q^{-1}F_b^{\rm ren}, \tag{55}$$

$$F_q^{\rm fin}=Z_q^{-1}F_q^{\rm ren}, \tag{56}$$

$$F_g^{\rm fin}=Z_g^{-1}F_g^{\rm ren}. \tag{57}$$

We stress that the factor $Z_q$ is the same for the $\gamma^*q\bar{q}$ and $Hb\bar{b}$ form factors. The fact that our explicit four-loop result for $F_b^{\rm fin}$ derived from Eq. (5) is indeed finite for $\epsilon \to 0$ is a nontrivial check of the pole subtraction framework and the involved anomalous dimensions.

Finally, we note that the scheme considered here is a *minimal* subtraction of just the poles in $\epsilon$ for $\ln F_r^{\rm ren}$, order-by-order in the coupling $a$. While the poles of $\ln F_r^{\rm ren}$ are equal to the poles of $\ln Z_r$ and thus are universal, due to exponentiation, the poles of $F_r^{\rm ren}$ at a given loop order are process dependent. In particular, their prediction based on (37) involves also higher order $\epsilon$ contributions from $F_r^{\rm ren}$ at lower loops.

## V. HARD MATCHING COEFFICIENTS IN SCET FROM $Hb\bar{b}$, $\gamma^* q\bar{q}$, AND $Hgg$ FORM FACTORS

In physical problems with widely separated scales the perturbative expansion can be spoiled since powers of the coupling are accompanied by powers of logarithms of large scale ratios. In such cases, the large logarithms can be resummed to all orders in perturbation theory by means of renormalization-group techniques formulated in the language of effective field theory. For the calculation of cross sections and kinematic distributions in collider physics the appropriate framework is provided by SCET [13–19], which is used, for instance, in Drell-Yan and Higgs production for rapidity [85–93], transverse-momentum [94–101], and thrust distributions [102–105], or for the treatment of threshold effects in deep-inelastic scattering (see, e.g., [106,107]). For all of these applications, the hard matching coefficients in SCET are required, which can be extracted from the form factors discussed above.

In dimensionally regularized SCET, the IR divergences in $F_r^{\rm ren}$, $r = b, q, g$, become the UV poles of the bare matching coefficients. In particular, performing the matching on-shell, loop integrals in SCET are scaleless and vanish; i.e., their UV and IR poles cancel each other. Furthermore, the IR poles must reproduce those of $F_r^{\rm ren}$, and hence we obtain the renormalized matching coefficients $C^r$ by subtracting the IR poles of $F_r^{\rm ren}$ through a multiplicative renormalization factor, which is precisely the procedure applied in Eqs. (55)–(57). We can therefore define the SCET hard matching coefficients $C^r$ for $r = b, q, g$ and their perturbative expansion according to

$$C^r = \lim_{\epsilon\to 0} F_r^{\rm fin} = 1 + \sum_{n=1}^{\infty} a^n C_n^r. \tag{58}$$

The matching coefficients depend on the renormalization scale $\mu$ through the renormalized coupling $a = a(\mu^2)$ and the logarithm $L$. Results through to three loops are available for $r = q, g$ in the literature [108], while to the best of our knowledge the full $Hb\bar{b}$ matching coefficient is presented here for the first time (the $L$-independent part through to three loops can be found in [89]).

We start with the matching coefficient for the $Hb\bar{b}$ form factor,

$$C_1^b = C_F[L^2(-1) + (\zeta_2 - 2)], \tag{59}$$

$$\begin{aligned} C_2^b = {}& C_F^2\left[L^4\left(\frac{1}{2}\right) + L^2(-\zeta_2 + 2) + L(24\zeta_3 - 12\zeta_2) + \left(-\frac{83}{10}\zeta_2^2 - 30\zeta_3 + 14\zeta_2 + 6\right)\right] \\ &+ C_F C_A\left[L^3\left(\frac{11}{9}\right) + L^2\left(2\zeta_2 - \frac{67}{9}\right) + L\left(-26\zeta_3 + \frac{22}{3}\zeta_2 + \frac{242}{27}\right) + \left(\frac{44}{5}\zeta_2^2 + \frac{151}{9}\zeta_3 - \frac{103}{18}\zeta_2 - \frac{467}{81}\right)\right] \\ &+ C_F n_f\left[L^3\left(-\frac{2}{9}\right) + L^2\left(\frac{10}{9}\right) + L\left(-\frac{4}{3}\zeta_2 - \frac{56}{27}\right) + \left(\frac{5}{9}\zeta_2 + \frac{2}{9}\zeta_3 + \frac{200}{81}\right)\right], \end{aligned} \tag{60}$$

$$\begin{aligned} C_3^b = {}& C_F^3\left[L^6\left(-\frac{1}{6}\right) + L^4\left(\frac{1}{2}\zeta_2 - 1\right) + L^3(-24\zeta_3 + 12\zeta_2) + L^2\left(\frac{83}{10}\zeta_2^2 + 30\zeta_3 - 14\zeta_2 - 6\right) + L\left(-240\zeta_5 - 8\zeta_3\zeta_2\right.\right. \\ &\left.\left. + \frac{228}{5}\zeta_2^2 + 20\zeta_3 + 42\zeta_2 - 50\right) + \left(16\zeta_3^2 + \frac{37729}{630}\zeta_2^3 + 424\zeta_5 + 178\zeta_3\zeta_2 - 77\zeta_2^2 - 654\zeta_3 - \frac{353}{3}\zeta_2 + \frac{575}{3}\right)\right] \\ &+ C_F^2 C_A\left[L^5\left(-\frac{11}{9}\right) + L^4\left(-2\zeta_2 + \frac{67}{9}\right) + L^3\left(26\zeta_3 - \frac{55}{9}\zeta_2 - \frac{308}{27}\right) + L^2\left(-\frac{34}{5}\zeta_2^2 - \frac{943}{9}\zeta_3 + \frac{689}{18}\zeta_2 + \frac{1673}{81}\right)\right. \\ &+ L\left(120\zeta_5 - 10\zeta_3\zeta_2 + 6\zeta_2^2 + \frac{1660}{3}\zeta_3 - \frac{7012}{27}\zeta_2 + \frac{614}{27}\right) + \left(\frac{296}{3}\zeta_3^2 - \frac{12676}{315}\zeta_2^3 - \frac{1676}{9}\zeta_5 - \frac{3049}{9}\zeta_3\zeta_2 - \frac{893}{270}\zeta_2^2\right. \\ &\left.\left. - \frac{4820}{27}\zeta_3 + \frac{31819}{81}\zeta_2 - \frac{9335}{81}\right)\right] + C_F C_A^2\left[L^4\left(-\frac{121}{54}\right) + L^3\left(-\frac{44}{9}\zeta_2 + \frac{1780}{81}\right) + L^2\left(-\frac{44}{5}\zeta_2^2 + 88\zeta_3\right.\right. \\ &\left. + \frac{26}{9}\zeta_2 - \frac{11939}{162}\right) + L\left(136\zeta_5 + \frac{88}{3}\zeta_3\zeta_2 - \frac{94}{3}\zeta_2^2 - \frac{13900}{27}\zeta_3 + \frac{9644}{81}\zeta_2 + \frac{10289}{1458}\right) \end{aligned}$$

$$+\left(-\frac{1136}{9}\zeta_3^2-\frac{6152}{189}\zeta_2^3+\frac{106}{9}\zeta_5+\frac{326}{3}\zeta_3\zeta_2+\frac{10093}{135}\zeta_2^2+\frac{107648}{243}\zeta_3-\frac{264515}{1458}\zeta_2+\frac{5964431}{26244}\right)\Bigg]$$
$$+n_fC_F^2\left[L^5\left(\frac{2}{9}\right)+L^4\left(-\frac{10}{9}\right)+L^3\left(\frac{10}{9}\zeta_2+\frac{50}{27}\right)+L^2\left(\frac{70}{9}\zeta_3-\frac{67}{9}\zeta_2+\frac{725}{162}\right)+L\left(\frac{28}{5}\zeta_2^2-\frac{832}{9}\zeta_3+\frac{880}{27}\zeta_2-\frac{1415}{54}\right)\right.$$
$$\left.+\left(-\frac{416}{9}\zeta_5-\frac{38}{9}\zeta_3\zeta_2-\frac{61}{27}\zeta_2^2+\frac{11996}{81}\zeta_3-\frac{6131}{162}\zeta_2+\frac{35875}{972}\right)\right]+n_fC_FC_A\left[L^4\left(\frac{22}{27}\right)+L^3\left(\frac{8}{9}\zeta_2-\frac{578}{81}\right)\right.$$
$$+L^2\left(-8\zeta_3+\frac{16}{3}\zeta_2+\frac{1727}{81}\right)+L\left(\frac{44}{15}\zeta_2^2+\frac{724}{9}\zeta_3-\frac{3272}{81}\zeta_2-\frac{7499}{729}\right)+\left(-\frac{4}{3}\zeta_5+\frac{4}{3}\zeta_3\zeta_2-\frac{476}{135}\zeta_2^2-\frac{2860}{27}\zeta_3\right.$$
$$\left.\left.+\frac{33259}{729}\zeta_2-\frac{521975}{13122}\right)\right]+n_f^2C_F\left[L^4\left(-\frac{2}{27}\right)+L^3\left(\frac{40}{81}\right)+L^2\left(-\frac{8}{9}\zeta_2-\frac{100}{81}\right)+L\left(\frac{16}{27}\zeta_3+\frac{80}{27}\zeta_2+\frac{928}{729}\right)\right.$$
$$\left.+\left(-\frac{188}{135}\zeta_2^2-\frac{200}{243}\zeta_3-\frac{212}{81}\zeta_2+\frac{2072}{6561}\right)\right],\tag{61}$$

$$C_4^b=C_F^4\left[L^8\left(\frac{1}{24}\right)+L^6\left(-\frac{1}{6}\zeta_2+\frac{1}{3}\right)+L^5(12\zeta_3-6\zeta_2)+L^4\left(-\frac{83}{20}\zeta_2^2-15\zeta_3+7\zeta_2+3\right)\right.$$
$$+L^3\left(240\zeta_5+8\zeta_3\zeta_2-\frac{228}{5}\zeta_2^2-20\zeta_3-42\zeta_2+50\right)+L^2\left(272\zeta_3^2-\frac{37729}{630}\zeta_2^3-424\zeta_5-466\zeta_3\zeta_2+149\zeta_2^2\right.$$
$$\left.+654\zeta_3+\frac{353}{3}\zeta_2-\frac{575}{3}\right)+L\left(5880\zeta_7-624\zeta_5\zeta_2-\frac{1028}{5}\zeta_3\zeta_2^2-1872\zeta_3^2-\frac{11386}{35}\zeta_2^3-2040\zeta_5+708\zeta_3\zeta_2\right.$$
$$\left.-402\zeta_2^2+2348\zeta_3-608\zeta_2+\frac{1382}{3}\right)+\left(-\frac{2208}{5}\zeta_{5,3}-1792\zeta_5\zeta_3+840\zeta_3^2\zeta_2-\frac{7508687}{63000}\zeta_2^4-\frac{12321}{2}\zeta_7\right.$$
$$\left.\left.-4448\zeta_5\zeta_2+\frac{2081}{5}\zeta_3\zeta_2^2+2940\zeta_3^2+\frac{31403}{45}\zeta_2^3+13323\zeta_5+292\zeta_3\zeta_2+\frac{972}{5}\zeta_2^2-9275\zeta_3+\frac{7029}{4}\zeta_2-\frac{22259}{12}\right)\right]$$
$$+C_F^3C_A\left[L^7\left(\frac{11}{18}\right)+L^6\left(\zeta_2-\frac{67}{18}\right)+L^5\left(-13\zeta_3+\frac{22}{9}\zeta_2+\frac{187}{27}\right)+L^4\left(\frac{12}{5}\zeta_2^2+\frac{2263}{18}\zeta_3-\frac{601}{12}\zeta_2-\frac{2879}{162}\right)\right.$$
$$+L^3\left(-120\zeta_5+58\zeta_3\zeta_2-\frac{3613}{90}\zeta_2^2-\frac{2306}{3}\zeta_3+\frac{9886}{27}\zeta_2-\frac{416}{27}\right)+L^2\left(-\frac{2168}{3}\zeta_3^2+\frac{7447}{315}\zeta_2^3+\frac{13556}{9}\zeta_5\right.$$
$$\left.+\frac{7693}{9}\zeta_3\zeta_2-\frac{7228}{27}\zeta_2^2+\frac{11312}{27}\zeta_3-\frac{63148}{81}\zeta_2+\frac{27992}{81}\right)+L\left(-10920\zeta_7+2184\zeta_5\zeta_2+\frac{2471}{5}\zeta_3\zeta_2^2+\frac{12680}{3}\zeta_3^2\right.$$
$$\left.+\frac{8969}{105}\zeta_2^3-5880\zeta_5-3404\zeta_3\zeta_2+\frac{258931}{135}\zeta_2^2+\frac{73226}{27}\zeta_3+\frac{8888}{3}\zeta_2-\frac{36350}{9}\right)+\left(-\frac{692}{5}\zeta_{5,3}+3696\zeta_5\zeta_3\right.$$
$$-\frac{8536}{3}\zeta_3^2\zeta_2+\frac{506012}{1125}\zeta_2^4+\frac{178357}{24}\zeta_7+\frac{83443}{9}\zeta_5\zeta_2-\frac{107401}{90}\zeta_3\zeta_2^2-2880\zeta_3^2+\frac{1145267}{3780}\zeta_2^3-\frac{73607}{36}\zeta_5$$
$$\left.\left.+\frac{320363}{54}\zeta_3\zeta_2-\frac{3878479}{1620}\zeta_2^2-\frac{526531}{36}\zeta_3-\frac{4901615}{648}\zeta_2+\frac{2888701}{216}\right)\right]+C_F^2C_A^2\left[L^6\left(\frac{242}{81}\right)+L^5\left(\frac{22}{3}\zeta_2-\frac{839}{27}\right)\right.$$
$$+L^4\left(\frac{54}{5}\zeta_2^2-\frac{1078}{9}\zeta_3-\frac{199}{18}\zeta_2+\frac{28393}{243}\right)+L^3\left(-136\zeta_5-\frac{244}{3}\zeta_3\zeta_2+\frac{778}{15}\zeta_2^2+\frac{85175}{81}\zeta_3-\frac{47353}{162}\zeta_2-\frac{181927}{1458}\right)$$
$$+L^2\left(\frac{4178}{9}\zeta_3^2+\frac{39076}{945}\zeta_2^3-\frac{6046}{9}\zeta_5-\frac{2392}{9}\zeta_3\zeta_2-\frac{13096}{135}\zeta_2^2-\frac{973523}{243}\zeta_3+\frac{2524883}{1458}\zeta_2-\frac{5785547}{26244}\right)$$
$$+L\left(8610\zeta_7-1968\zeta_5\zeta_2-\frac{3184}{15}\zeta_3\zeta_2^2-\frac{35000}{9}\zeta_3^2-\frac{17506}{315}\zeta_2^3+\frac{5794}{3}\zeta_5+\frac{11527}{3}\zeta_3\zeta_2-\frac{284933}{405}\zeta_2^2+\frac{2079788}{243}\zeta_3\right.$$
$$\left.-\frac{9736801}{1458}\zeta_2+\frac{6576527}{2187}\right)+\left(1046\zeta_{5,3}-5104\zeta_5\zeta_3+\frac{24208}{9}\zeta_3^2\zeta_2-\frac{3829877}{4725}\zeta_2^4-\frac{105405}{16}\zeta_7-\frac{91561}{18}\zeta_5\zeta_2\right.$$

$$
\begin{aligned}
&+\frac{64541}{45}\zeta_3\zeta_2^2+\frac{697187}{81}\zeta_3^2+\frac{113683}{1260}\zeta_2^3-\frac{125555}{216}\zeta_5-\frac{12580021}{972}\zeta_3\zeta_2+\frac{52786259}{29160}\zeta_2^2+\frac{29217731}{5832}\zeta_3\\
&+\frac{279041783}{26244}\zeta_2-\frac{526960807}{52488}\bigg)\bigg]+C_FC_A^3\bigg[L^5\left(\frac{1331}{270}\right)+L^4\left(\frac{121}{9}\zeta_2-\frac{5456}{81}\right)\\
&+L^3\left(\frac{484}{15}\zeta_2^2-\frac{968}{3}\zeta_3-\frac{694}{27}\zeta_2+\frac{83618}{243}\right)+L^2\bigg(4\zeta_3^2+\frac{5008}{105}\zeta_2^3-\frac{5830}{9}\zeta_5-132\zeta_3\zeta_2-\frac{121}{15}\zeta_2^2+\frac{26390}{9}\zeta_3\\
&-\frac{4186}{9}\zeta_2-\frac{1167889}{2916}\bigg)+L\bigg(-\frac{45511}{12}\zeta_7+\frac{824}{3}\zeta_5\zeta_2-\frac{2066}{15}\zeta_3\zeta_2^2+\frac{15059}{9}\zeta_3^2+\frac{222632}{945}\zeta_2^3+\frac{95965}{27}\zeta_5-\frac{3058}{9}\zeta_3\zeta_2\\
&-\frac{2972}{9}\zeta_2^2-\frac{243382}{27}\zeta_3+\frac{1361261}{486}\zeta_2-\frac{27115865}{8748}\bigg)+\bigg(-\frac{14161}{30}\zeta_{5,3}+\frac{21577}{6}\zeta_5\zeta_3-\frac{1963}{3}\zeta_3^2\zeta_2+\frac{10233079}{15750}\zeta_2^4\\
&+\frac{258199}{144}\zeta_7+1056\zeta_5\zeta_2-\frac{23288}{45}\zeta_3\zeta_2^2-\frac{702221}{108}\zeta_3^2-\frac{2000759}{2268}\zeta_2^3-\frac{9786737}{3240}\zeta_5+\frac{444085}{108}\zeta_3\zeta_2+\frac{184637}{810}\zeta_2^2\\
&+\frac{8121343}{1458}\zeta_3-\frac{146447531}{34992}\zeta_2+\frac{3966128773}{419904}\bigg)\bigg]+\frac{d_F^{abcd}d_A^{abcd}}{N_F}\bigg[L^2\left(96\zeta_3^2+\frac{1984}{35}\zeta_2^3-\frac{880}{3}\zeta_5-\frac{32}{3}\zeta_3+32\zeta_2\right)\\
&+L\left(1742\zeta_7+512\zeta_5\zeta_2-\frac{368}{5}\zeta_3\zeta_2^2-\frac{1672}{3}\zeta_3^2+\frac{13904}{315}\zeta_2^3-\frac{920}{9}\zeta_5-896\zeta_3\zeta_2+\frac{112}{15}\zeta_2^2-\frac{6064}{9}\zeta_3-\frac{1088}{3}\zeta_2+128\right)\\
&+\bigg(260\zeta_{5,3}-5092\zeta_5\zeta_3-16\zeta_3^2\zeta_2-\frac{496766}{525}\zeta_2^4-1228\zeta_7-\frac{12808}{3}\zeta_5\zeta_2+\frac{14216}{15}\zeta_3\zeta_2^2+\frac{72674}{9}\zeta_3^2+\frac{768632}{945}\zeta_2^3\\
&-\frac{65546}{27}\zeta_5+\frac{2516}{3}\zeta_3\zeta_2+\frac{8692}{45}\zeta_2^2+\frac{112346}{27}\zeta_3+\frac{8194}{9}\zeta_2-\frac{1588}{3}\bigg)\bigg]+n_fC_F^3\bigg[L^7\left(-\frac{1}{9}\right)+L^6\left(\frac{5}{9}\right)\\
&+L^5\left(-\frac{4}{9}\zeta_2-\frac{22}{27}\right)+L^4\left(-\frac{119}{9}\zeta_3+\frac{59}{6}\zeta_2-\frac{925}{162}\right)+L^3\left(-\frac{169}{45}\zeta_2^2+\frac{1132}{9}\zeta_3-\frac{1342}{27}\zeta_2+\frac{1433}{54}\right)\\
&+L^2\left(-\frac{1024}{9}\zeta_5-\frac{466}{9}\zeta_3\zeta_2+\frac{7916}{135}\zeta_2^2-\frac{14624}{81}\zeta_3+\frac{7894}{81}\zeta_2-\frac{111259}{972}\right)+L\bigg(\frac{664}{3}\zeta_3^2-\frac{3278}{105}\zeta_2^3+\frac{5200}{3}\zeta_5\\
&+\frac{2600}{9}\zeta_3\zeta_2-\frac{8402}{27}\zeta_2^2-\frac{42656}{27}\zeta_3-\frac{6499}{54}\zeta_2+\frac{46391}{72}\bigg)+\bigg(\frac{2013}{2}\zeta_7-\frac{1124}{9}\zeta_5\zeta_2-\frac{7567}{45}\zeta_3\zeta_2^2-\frac{3764}{3}\zeta_3^2\\
&-\frac{107227}{1890}\zeta_2^3-\frac{70907}{18}\zeta_5-\frac{72811}{81}\zeta_3\zeta_2+\frac{432143}{810}\zeta_2^2+\frac{1934375}{324}\zeta_3+\frac{172627}{972}\zeta_2-\frac{6554087}{3888}\bigg)\bigg]\\
&+n_fC_F^2C_A\bigg[L^6\left(-\frac{88}{81}\right)+L^5\left(-\frac{4}{3}\zeta_2+\frac{274}{27}\right)+L^4\left(\frac{124}{9}\zeta_3-\frac{50}{9}\zeta_2-\frac{15889}{486}\right)+L^3\bigg(-\frac{20}{3}\zeta_2^2-\frac{16264}{81}\zeta_3\\
&+\frac{8804}{81}\zeta_2+\frac{5047}{729}\bigg)+L^2\left(\frac{244}{3}\zeta_5+\frac{664}{9}\zeta_3\zeta_2-\frac{1606}{135}\zeta_2^2+\frac{91328}{81}\zeta_3-\frac{408010}{729}\zeta_2+\frac{7464559}{26244}\right)\\
&+L\left(-\frac{3376}{9}\zeta_3^2-\frac{1564}{63}\zeta_2^3-\frac{1948}{3}\zeta_5-\frac{10802}{27}\zeta_3\zeta_2+\frac{177476}{405}\zeta_2^2-\frac{642457}{243}\zeta_3+\frac{2079563}{1458}\zeta_2-\frac{18844181}{17496}\right)\\
&+\bigg(-\frac{1219}{4}\zeta_7+114\zeta_5\zeta_2+\frac{15934}{45}\zeta_3\zeta_2^2+\frac{9446}{81}\zeta_3^2-\frac{1846}{21}\zeta_2^3+\frac{45995}{18}\zeta_5+\frac{155563}{81}\zeta_3\zeta_2-\frac{3347782}{3645}\zeta_2^2\\
&-\frac{1262017}{5832}\zeta_3-\frac{145213765}{104976}\zeta_2+\frac{756958495}{419904}\bigg)\bigg]+n_fC_FC_A^2\bigg[L^5\left(-\frac{121}{45}\right)+L^4\left(-\frac{44}{9}\zeta_2+\frac{1831}{54}\right)\\
&+L^3\left(-\frac{88}{15}\zeta_2^2+88\zeta_3-\frac{356}{27}\zeta_2-\frac{8693}{54}\right)+L^2\left(\frac{700}{9}\zeta_5-8\zeta_3\zeta_2-\frac{208}{5}\zeta_2^2-830\zeta_3+\frac{8588}{27}\zeta_2+\frac{186151}{972}\right)\\
&+L\left(\frac{1186}{9}\zeta_3^2-\frac{25244}{945}\zeta_2^3-\frac{1324}{27}\zeta_5+\frac{32}{9}\zeta_3\zeta_2+\frac{52}{15}\zeta_2^2+\frac{234470}{81}\zeta_3-\frac{290270}{243}\zeta_2+\frac{12030185}{11664}\right)\\
&+\bigg(\frac{19141}{72}\zeta_7-\frac{127}{3}\zeta_5\zeta_2-\frac{6904}{45}\zeta_3\zeta_2^2+\frac{5462}{9}\zeta_3^2+\frac{153371}{2268}\zeta_2^3-\frac{2343853}{3240}\zeta_5-\frac{73985}{108}\zeta_3\zeta_2+\frac{120913}{540}\zeta_2^2
\end{aligned}
$$

$$
-\frac{16605365}{5832}\zeta_3+\frac{46423375}{34992}\zeta_2-\frac{2567430839}{839808}\bigg)\bigg]+n_f\frac{d_F^{abcd}d_F^{abcd}}{N_F}\bigg[L^2\bigg(\frac{320}{3}\zeta_5+\frac{64}{3}\zeta_3-64\zeta_2\bigg)
+L\bigg(\frac{608}{3}\zeta_3^2+\frac{4736}{315}\zeta_2^3-\frac{10880}{9}\zeta_5+64\zeta_3\zeta_2-\frac{160}{3}\zeta_2^2+\frac{1664}{9}\zeta_3+\frac{2272}{3}\zeta_2-256\bigg)+\bigg(-1240\zeta_7+\frac{992}{3}\zeta_5\zeta_2
-\frac{3952}{15}\zeta_3\zeta_2^2-\frac{4504}{9}\zeta_3^2+\frac{215876}{945}\zeta_2^3+\frac{101938}{27}\zeta_5+\frac{572}{3}\zeta_3\zeta_2-\frac{8}{45}\zeta_2^2-\frac{18202}{27}\zeta_3-\frac{18254}{9}\zeta_2+\frac{3488}{3}\bigg)\bigg]
+n_f^2C_F^2\bigg[L^6\bigg(\frac{8}{81}\bigg)+L^5\bigg(-\frac{20}{27}\bigg)+L^4\bigg(\frac{10}{9}\zeta_2+\frac{463}{243}\bigg)+L^3\bigg(\frac{380}{81}\zeta_3-\frac{254}{27}\zeta_2+\frac{2104}{729}\bigg)
+L^2\bigg(\frac{692}{135}\zeta_2^2-\frac{17884}{243}\zeta_3+\frac{2906}{81}\zeta_2-\frac{457105}{13122}\bigg)+L\bigg(-\frac{104}{3}\zeta_5-\frac{568}{27}\zeta_3\zeta_2-\frac{1924}{45}\zeta_2^2+\frac{75380}{243}\zeta_3-\frac{36440}{729}\zeta_2+\frac{837923}{8748}\bigg)
+\bigg(\frac{4556}{81}\zeta_3^2+\frac{3520}{189}\zeta_2^3-\frac{1568}{27}\zeta_5+\frac{3358}{243}\zeta_3\zeta_2+\frac{45551}{810}\zeta_2^2-\frac{612127}{1458}\zeta_3+\frac{74333}{6561}\zeta_2-\frac{11290865}{104976}\bigg)\bigg]
+n_f^2C_FC_A\bigg[L^5\bigg(\frac{22}{45}\bigg)+L^4\bigg(\frac{4}{9}\zeta_2-\frac{143}{27}\bigg)+L^3\bigg(-\frac{16}{3}\zeta_3+\frac{184}{27}\zeta_2+\frac{3515}{162}\bigg)+L^2\bigg(\frac{20}{3}\zeta_2^2+\frac{508}{9}\zeta_3-\frac{1600}{27}\zeta_2-\frac{26293}{972}\bigg)
+L\bigg(-\frac{616}{9}\zeta_5+\frac{152}{9}\zeta_3\zeta_2+\frac{344}{15}\zeta_2^2-\frac{17068}{81}\zeta_3+\frac{36643}{243}\zeta_2-\frac{823055}{11664}\bigg)+\bigg(-\frac{622}{27}\zeta_3^2+\frac{1654}{135}\zeta_2^3+\frac{19094}{135}\zeta_5
-\frac{20}{27}\zeta_3\zeta_2-\frac{1957}{27}\zeta_2^2+\frac{408781}{1458}\zeta_3-\frac{4264925}{34992}\zeta_2+\frac{176182813}{839808}\bigg)\bigg]+n_f^3C_F\bigg[L^5\bigg(-\frac{4}{135}\bigg)+L^4\bigg(\frac{20}{81}\bigg)
+L^3\bigg(-\frac{16}{27}\zeta_2-\frac{200}{243}\bigg)+L^2\bigg(\frac{80}{27}\zeta_2+\frac{1000}{729}\bigg)+L\bigg(-\frac{104}{45}\zeta_2^2-\frac{40}{81}\zeta_3-\frac{400}{81}\zeta_2-\frac{2608}{2187}\bigg)
+\bigg(-\frac{106}{135}\zeta_5+\frac{4}{9}\zeta_3\zeta_2+\frac{328}{81}\zeta_2^2+\frac{14}{243}\zeta_3+\frac{1946}{729}\zeta_2+\frac{6460}{6561}\bigg)\bigg]. \tag{62}
$$

In the case of the $\gamma^* q\bar{q}$ form factor, the lower-loop results can be found in [108], and we use the same normalization here. The four-loop result can be extracted from $F_q^{(4)}$ in Ref. [65] and reads

$$
C_4^q=C_F^4\bigg[L^8\bigg(\frac{1}{24}\bigg)+L^7\bigg(-\frac{1}{2}\bigg)+L^6\bigg(-\frac{1}{6}\zeta_2+\frac{43}{12}\bigg)+L^5\bigg(12\zeta_3-\frac{9}{2}\zeta_2-\frac{63}{4}\bigg)+L^4\bigg(-\frac{83}{20}\zeta_2^2-87\zeta_3+42\zeta_2+\frac{813}{16}\bigg)
+L^3\bigg(240\zeta_5+8\zeta_3\zeta_2-\frac{207}{10}\zeta_2^2+322\zeta_3-228\zeta_2-\frac{1019}{8}\bigg)+L^2\bigg(272\zeta_3^2-\frac{37729}{630}\zeta_2^3-1384\zeta_5-562\zeta_3\zeta_2
+\frac{5081}{20}\zeta_2^2-\zeta_3+\frac{16603}{24}\zeta_2+\frac{17455}{48}\bigg)+L\bigg(5880\zeta_7-624\zeta_5\zeta_2-\frac{1028}{5}\zeta_3\zeta_2^2-1824\zeta_3^2-\frac{30587}{210}\zeta_2^3+1392\zeta_5
+1818\zeta_3\zeta_2-\frac{21837}{20}\zeta_2^2+770\zeta_3-\frac{13895}{8}\zeta_2-\frac{23995}{48}\bigg)+\bigg(-\frac{2208}{5}\zeta_{5,3}-1792\zeta_5\zeta_3+840\zeta_3^2\zeta_2-\frac{7508687}{63000}\zeta_2^4
-\frac{29919}{2}\zeta_7-2696\zeta_5\zeta_2+\frac{2009}{5}\zeta_3\zeta_2^2+5072\zeta_3^2+\frac{563503}{630}\zeta_2^3+\frac{44977}{3}\zeta_5-1930\zeta_3\zeta_2+\frac{19375}{16}\zeta_2^2-\frac{129505}{12}\zeta_3
+\frac{26749}{8}\zeta_2+\frac{153365}{384}\bigg)\bigg]+C_F^3C_A\bigg[L^7\bigg(\frac{11}{18}\bigg)+L^6\bigg(\zeta_2-\frac{365}{36}\bigg)+L^5\bigg(-13\zeta_3-\frac{32}{9}\zeta_2+\frac{8389}{108}\bigg)
+L^4\bigg(\frac{12}{5}\zeta_2^2+\frac{3829}{18}\zeta_3-\frac{581}{12}\zeta_2-\frac{472609}{1296}\bigg)+L^3\bigg(-120\zeta_5+58\zeta_3\zeta_2-\frac{5449}{90}\zeta_2^2-1542\zeta_3+\frac{36677}{54}\zeta_2+1101\bigg)
+L^2\bigg(-\frac{2168}{3}\zeta_3^2+\frac{7447}{315}\zeta_2^3+\frac{17876}{9}\zeta_5+\frac{8125}{9}\zeta_3\zeta_2-\frac{14629}{108}\zeta_2^2+\frac{258667}{54}\zeta_3-\frac{2084963}{648}\zeta_2-\frac{1547747}{648}\bigg)
+L\bigg(-10920\zeta_7+2184\zeta_5\zeta_2+\frac{2471}{5}\zeta_3\zeta_2^2+\frac{14864}{3}\zeta_3^2-\frac{3707}{105}\zeta_2^3-\frac{30476}{3}\zeta_5-\frac{18757}{3}\zeta_3\zeta_2+\frac{1313227}{540}\zeta_2^2
$$

$$
\begin{aligned}
&-\frac{608191}{108}\zeta_3+\frac{676297}{72}\zeta_2+\frac{46493}{12}\bigg)+\bigg(-\frac{692}{5}\zeta_{5,3}+3696\zeta_5\zeta_3-\frac{8536}{3}\zeta_3^2\zeta_2+\frac{506012}{1125}\zeta_2^4+\frac{474205}{24}\zeta_7\\
&+\frac{37975}{9}\zeta_5\zeta_2-\frac{113287}{90}\zeta_3\zeta_2^2-8504\zeta_3^2+\frac{2013857}{3780}\zeta_2^3+\frac{325717}{36}\zeta_5+\frac{787613}{54}\zeta_3\zeta_2-\frac{32251333}{6480}\zeta_2^2-\frac{288281}{72}\zeta_3\\
&-\frac{6575143}{432}\zeta_2-\frac{1147289}{192}\bigg)\bigg]+C_F^2C_A^2\bigg[L^6\bigg(\frac{242}{81}\bigg)+L^5\bigg(\frac{22}{3}\zeta_2-\frac{1565}{27}\bigg)+L^4\bigg(\frac{54}{5}\zeta_2^2-\frac{1078}{9}\zeta_3-\frac{661}{18}\zeta_2+\frac{964631}{1944}\bigg)\\
&+L^3\bigg(-136\zeta_5-\frac{244}{3}\zeta_3\zeta_2+\frac{382}{15}\zeta_2^2+\frac{130616}{81}\zeta_3-\frac{51205}{162}\zeta_2-\frac{13874701}{5832}\bigg)+L^2\bigg(\frac{4178}{9}\zeta_3^2+\frac{39076}{945}\zeta_2^3-\frac{1834}{9}\zeta_5\\
&-\frac{1546}{9}\zeta_3\zeta_2-\frac{11875}{54}\zeta_2^2-\frac{2038430}{243}\zeta_3+\frac{2509531}{729}\zeta_2+\frac{721539817}{104976}\bigg)+L\bigg(8610\zeta_7-1968\zeta_5\zeta_2-\frac{3184}{15}\zeta_3\zeta_2^2\\
&-\frac{42620}{9}\zeta_3^2-\frac{48266}{315}\zeta_2^3+\frac{8192}{3}\zeta_5+\frac{16429}{3}\zeta_3\zeta_2-\frac{398749}{810}\zeta_2^2+\frac{21435407}{972}\zeta_3-\frac{21743419}{1458}\zeta_2-\frac{407701829}{34992}\bigg)\\
&+\bigg(1046\zeta_{5,3}-5104\zeta_5\zeta_3+\frac{24208}{9}\zeta_3^2\zeta_2-\frac{3829877}{4725}\zeta_2^4-\frac{248037}{16}\zeta_7-\frac{6781}{18}\zeta_5\zeta_2+\frac{64919}{45}\zeta_3\zeta_2^2+\frac{1022996}{81}\zeta_3^2\\
&-\frac{103553}{420}\zeta_2^3-\frac{1113539}{216}\zeta_5-\frac{20087587}{972}\zeta_3\zeta_2+\frac{95100011}{29160}\zeta_2^2-\frac{51597389}{2916}\zeta_3+\frac{2779278167}{104976}\zeta_2+\frac{9643400117}{839808}\bigg)\bigg]\\
&+C_FC_A^3\bigg[L^5\bigg(\frac{1331}{270}\bigg)+L^4\bigg(\frac{121}{9}\zeta_2-\frac{33803}{324}\bigg)+L^3\bigg(\frac{484}{15}\zeta_2^2-\frac{968}{3}\zeta_3-\frac{694}{27}\zeta_2+\frac{467107}{486}\bigg)\\
&+L^2\bigg(4\zeta_3^2+\frac{5008}{105}\zeta_2^3-\frac{5830}{9}\zeta_5-132\zeta_3\zeta_2-\frac{121}{15}\zeta_2^2+\frac{32924}{9}\zeta_3-\frac{8905}{9}\zeta_2-\frac{3513241}{729}\bigg)\\
&+L\bigg(-\frac{45511}{12}\zeta_7+\frac{824}{3}\zeta_5\zeta_2-\frac{2066}{15}\zeta_3\zeta_2^2+\frac{15059}{9}\zeta_3^2+\frac{222632}{945}\zeta_2^3+\frac{101905}{27}\zeta_5-\frac{6028}{9}\zeta_3\zeta_2-\frac{36947}{90}\zeta_2^2\\
&-\frac{854477}{54}\zeta_3+\frac{1779112}{243}\zeta_2+\frac{114204817}{8748}\bigg)+\bigg(-\frac{14161}{30}\zeta_{5,3}+\frac{21577}{6}\zeta_5\zeta_3-\frac{1963}{3}\zeta_3^2\zeta_2+\frac{10233079}{15750}\zeta_2^4\\
&+\frac{616417}{144}\zeta_7-397\zeta_5\zeta_2-\frac{19823}{45}\zeta_3\zeta_2^2-\frac{845393}{108}\zeta_3^2-\frac{8189719}{11340}\zeta_2^3-\frac{8979437}{3240}\zeta_5+\frac{720313}{108}\zeta_3\zeta_2-\frac{283307}{1620}\zeta_2^2\\
&+\frac{32942281}{1458}\zeta_3-\frac{540427967}{34992}\zeta_2-\frac{3289233097}{209952}\bigg)\bigg]+\frac{d_F^{abcd}d_A^{abcd}}{N_F}\bigg[L^2\bigg(96\zeta_3^2+\frac{1984}{35}\zeta_2^3-\frac{880}{3}\zeta_5-\frac{32}{3}\zeta_3+32\zeta_2\bigg)\\
&+L\bigg(1742\zeta_7+512\zeta_5\zeta_2-\frac{368}{5}\zeta_3\zeta_2^2-\frac{1672}{3}\zeta_3^2+\frac{13904}{315}\zeta_2^3-\frac{920}{9}\zeta_5-896\zeta_3\zeta_2+\frac{112}{15}\zeta_2^2-\frac{3904}{9}\zeta_3-\frac{1088}{3}\zeta_2+96\bigg)\\
&+\bigg(260\zeta_{5,3}-5092\zeta_5\zeta_3-16\zeta_3^2\zeta_2-\frac{496766}{525}\zeta_2^4+3518\zeta_7-\frac{4744}{3}\zeta_5\zeta_2+\frac{6584}{15}\zeta_3\zeta_2^2+\frac{39986}{9}\zeta_3^2+\frac{526496}{945}\zeta_2^3\\
&-\frac{180566}{27}\zeta_5+\frac{3020}{3}\zeta_3\zeta_2+\frac{1220}{9}\zeta_2^2+\frac{169532}{27}\zeta_3+\frac{10570}{9}\zeta_2-\frac{1580}{3}\bigg)\bigg]+n_fC_F^3\bigg[L^7\bigg(-\frac{1}{9}\bigg)+L^6\bigg(\frac{31}{18}\bigg)\\
&+L^5\bigg(-\frac{4}{9}\zeta_2-\frac{665}{54}\bigg)+L^4\bigg(-\frac{119}{9}\zeta_3+\frac{79}{6}\zeta_2+\frac{29645}{648}\bigg)+L^3\bigg(-\frac{169}{45}\zeta_2^2+\frac{1342}{9}\zeta_3-\frac{3085}{27}\zeta_2-\frac{1975}{27}\bigg)\\
&+L^2\bigg(-\frac{1024}{9}\zeta_5-\frac{466}{9}\zeta_3\zeta_2+\frac{20827}{270}\zeta_2^2-\frac{49697}{81}\zeta_3+\frac{153121}{324}\zeta_2-\frac{15028}{243}\bigg)+L\bigg(\frac{664}{3}\zeta_3^2-\frac{3278}{105}\zeta_2^3+\frac{5504}{3}\zeta_5\\
&+\frac{4430}{9}\zeta_3\zeta_2-\frac{133739}{270}\zeta_2^2-\frac{281}{9}\zeta_3-\frac{105101}{108}\zeta_2+\frac{225611}{648}\bigg)+\bigg(\frac{2013}{2}\zeta_7-\frac{1124}{9}\zeta_5\zeta_2-\frac{7567}{45}\zeta_3\zeta_2^2-\frac{3032}{3}\zeta_3^2\\
&-\frac{20477}{378}\zeta_2^3-\frac{105215}{18}\zeta_5-\frac{113617}{81}\zeta_3\zeta_2+\frac{3288893}{3240}\zeta_2^2+\frac{802207}{162}\zeta_3+\frac{1539611}{1944}\zeta_2-\frac{1841095}{7776}\bigg)\bigg]
\end{aligned}
$$

$$
\begin{aligned}
&+n_f C_F^2 C_A\Bigg[L^6\left(-\frac{88}{81}\right)+L^5\left(-\frac{4}{3}\zeta_2+\frac{538}{27}\right)+L^4\left(\frac{124}{9}\zeta_3-\frac{8}{9}\zeta_2-\frac{38720}{243}\right)+L^3\left(-\frac{20}{3}\zeta_2^2-\frac{20638}{81}\zeta_3\right.\\
&\left.+\frac{12566}{81}\zeta_2+\frac{500083}{729}\right)+L^2\left(\frac{244}{3}\zeta_5+\frac{664}{9}\zeta_3\zeta_2+\frac{824}{135}\zeta_2^2+\frac{124628}{81}\zeta_3-\frac{1743011}{1458}\zeta_2-\frac{39939557}{26244}\right)\\
&+L\left(-\frac{3376}{9}\zeta_3^2-\frac{1564}{63}\zeta_2^3-\frac{2560}{3}\zeta_5-\frac{17930}{27}\zeta_3\zeta_2+\frac{223466}{405}\zeta_2^2-\frac{2214461}{486}\zeta_3+\frac{5773673}{1458}\zeta_2+\frac{20234099}{17496}\right)\\
&+\left(-\frac{1219}{4}\zeta_7+114\zeta_5\zeta_2+\frac{15934}{45}\zeta_3\zeta_2^2+\frac{10904}{81}\zeta_3^2-\frac{808}{105}\zeta_2^3+\frac{44981}{18}\zeta_5+\frac{189565}{81}\zeta_3\zeta_2-\frac{6376939}{3645}\zeta_2^2\right.\\
&\left.+\frac{25114571}{5832}\zeta_3-\frac{547858717}{104976}\zeta_2+\frac{273777229}{419904}\right)\Bigg]+n_f C_F C_A^2\Bigg[L^5\left(-\frac{121}{45}\right)+L^4\left(-\frac{44}{9}\zeta_2+\frac{1460}{27}\right)\\
&+L^3\left(-\frac{88}{15}\zeta_2^2+88\zeta_3-\frac{356}{27}\zeta_2-\frac{25553}{54}\right)+L^2\left(\frac{700}{9}\zeta_5-8\zeta_3\zeta_2-\frac{208}{5}\zeta_2^2-962\zeta_3+\frac{15914}{27}\zeta_2+\frac{545491}{243}\right)\\
&+L\left(\frac{1186}{9}\zeta_3^2-\frac{25244}{945}\zeta_2^3+\frac{836}{27}\zeta_5+\frac{572}{9}\zeta_3\zeta_2+\frac{469}{15}\zeta_2^2+\frac{351677}{81}\zeta_3-\frac{810803}{243}\zeta_2-\frac{66887935}{11664}\right)\\
&+\left(\frac{19141}{72}\zeta_7-\frac{127}{3}\zeta_5\zeta_2-\frac{6904}{45}\zeta_3\zeta_2^2+\frac{4958}{9}\zeta_3^2+\frac{345871}{11340}\zeta_2^3-\frac{3862513}{3240}\zeta_5-\frac{92201}{108}\zeta_3\zeta_2+\frac{316999}{540}\zeta_2^2\right.\\
&\left.-\frac{40209899}{5832}\zeta_3+\frac{213890551}{34992}\zeta_2+\frac{5309402065}{839808}\right)\Bigg]+n_f\frac{d_F^{abcd}d_F^{abcd}}{N_F}\Bigg[L^2\left(\frac{320}{3}\zeta_5+\frac{64}{3}\zeta_3-64\zeta_2\right)\\
&+L\left(\frac{608}{3}\zeta_3^2+\frac{4736}{315}\zeta_2^3-\frac{10880}{9}\zeta_5+64\zeta_3\zeta_2-\frac{160}{3}\zeta_2^2-\frac{2656}{9}\zeta_3+\frac{2272}{3}\zeta_2-192\right)+\left(-1240\zeta_7+\frac{992}{3}\zeta_5\zeta_2\right.\\
&\left.-\frac{3952}{15}\zeta_3\zeta_2^2+\frac{680}{9}\zeta_3^2+\frac{41620}{189}\zeta_2^3+\frac{95098}{27}\zeta_5+\frac{92}{3}\zeta_3\zeta_2+\frac{7552}{45}\zeta_2^2-\frac{13414}{27}\zeta_3-\frac{21566}{9}\zeta_2+\frac{3190}{3}\right)\Bigg]\\
&+n_{q\gamma}C_F\frac{d_F^{abc}d_F^{abc}}{N_F}\Bigg[L^2\left(\frac{640}{3}\zeta_5+\frac{16}{5}\zeta_2^2-\frac{112}{3}\zeta_3-80\zeta_2-32\right)+L\left(-640\zeta_5-\frac{48}{5}\zeta_2^2+112\zeta_3+240\zeta_2+96\right)\\
&+\left(\frac{11536}{3}\zeta_7+\frac{1280}{3}\zeta_5\zeta_2+\frac{1408}{5}\zeta_3\zeta_2^2-672\zeta_3^2-\frac{25808}{105}\zeta_2^3+\frac{10160}{3}\zeta_5-\frac{2672}{3}\zeta_3\zeta_2-\frac{1392}{5}\zeta_2^2-\frac{2752}{3}\zeta_3\right.\\
&\left.-1376\zeta_2-\frac{7040}{9}\right)\Bigg]+n_{q\gamma}C_A\frac{d_F^{abc}d_F^{abc}}{N_F}\Bigg[L\left(\frac{7040}{3}\zeta_5+\frac{176}{5}\zeta_2^2-\frac{1232}{3}\zeta_3-880\zeta_2-352\right)\\
&+\left(-\frac{13972}{3}\zeta_7-1840\zeta_5\zeta_2-\frac{784}{5}\zeta_3\zeta_2^2-\frac{8752}{3}\zeta_3^2-\frac{523448}{945}\zeta_2^3-\frac{11740}{9}\zeta_5+\frac{7192}{3}\zeta_3\zeta_2-\frac{43948}{45}\zeta_2^2+\frac{12568}{3}\zeta_3\right.\\
&\left.+\frac{39344}{9}\zeta_2+\frac{20384}{9}\right)\Bigg]+n_f^2 C_F^2\Bigg[L^6\left(\frac{8}{81}\right)+L^5\left(-\frac{44}{27}\right)+L^4\left(\frac{10}{9}\zeta_2+\frac{5741}{486}\right)+L^3\left(\frac{380}{81}\zeta_3-\frac{434}{27}\zeta_2-\frac{62959}{1458}\right)\\
&+L^2\left(\frac{692}{135}\zeta_2^2-\frac{11350}{243}\zeta_3+\frac{7415}{81}\zeta_2+\frac{1473913}{26244}\right)+L\left(-\frac{104}{3}\zeta_5-\frac{568}{27}\zeta_3\zeta_2-\frac{184}{3}\zeta_2^2+\frac{71018}{243}\zeta_3\right.\\
&\left.-\frac{170090}{729}\zeta_2+\frac{235108}{2187}\right)+\left(\frac{4556}{81}\zeta_3^2+\frac{3520}{189}\zeta_2^3+\frac{3796}{27}\zeta_5+\frac{18802}{243}\zeta_3\zeta_2+\frac{107507}{810}\zeta_2^2-\frac{514580}{729}\zeta_3\right.\\
&\left.+\frac{5818805}{26244}\zeta_2-\frac{73476853}{209952}\right)\Bigg]+n_f^2 C_F C_A\Bigg[L^5\left(\frac{22}{45}\right)+L^4\left(\frac{4}{9}\zeta_2-\frac{242}{27}\right)+L^3\left(-\frac{16}{3}\zeta_3+\frac{184}{27}\zeta_2+\frac{11651}{162}\right)\\
&+L^2\left(\frac{20}{3}\zeta_2^2+\frac{508}{9}\zeta_3-\frac{2860}{27}\zeta_2-\frac{154343}{486}\right)+L\left(-\frac{616}{9}\zeta_5+\frac{152}{9}\zeta_3\zeta_2+\frac{308}{15}\zeta_2^2-\frac{21604}{81}\zeta_3+\frac{114943}{243}\zeta_2+\frac{8996449}{11664}\right)\\
&+\left(-\frac{622}{27}\zeta_3^2+\frac{1654}{135}\zeta_2^3+\frac{22874}{135}\zeta_5-\frac{956}{27}\zeta_3\zeta_2-\frac{18431}{135}\zeta_2^2+\frac{719659}{1458}\zeta_3-\frac{26318309}{34992}\zeta_2-\frac{689230799}{839808}\right)\Bigg]
\end{aligned}
$$

$$
\begin{aligned}
&+n_{q\gamma}n_f\frac{d_F^{abc}d_F^{abc}}{N_F}\left[L\left(-\frac{1280}{3}\zeta_5-\frac{32}{5}\zeta_2^2+\frac{224}{3}\zeta_3+160\zeta_2+64\right)+\left(\frac{1408}{3}\zeta_3^2+\frac{11264}{135}\zeta_2^3+\frac{3520}{9}\zeta_5-\frac{448}{3}\zeta_3\zeta_2\right.\right.\\
&\left.\left.+\frac{608}{9}\zeta_2^2-224\zeta_3-\frac{4448}{9}\zeta_2-\frac{3136}{9}\right)\right]+n_f^3C_F\left[L^5\left(-\frac{4}{135}\right)+L^4\left(\frac{38}{81}\right)+L^3\left(-\frac{16}{27}\zeta_2-\frac{812}{243}\right)\right.\\
&+L^2\left(\frac{152}{27}\zeta_2+\frac{9910}{729}\right)+L\left(-\frac{104}{45}\zeta_2^2-\frac{40}{81}\zeta_3-\frac{1624}{81}\zeta_2-\frac{69874}{2187}\right)+\left(-\frac{106}{135}\zeta_5+\frac{4}{9}\zeta_3\zeta_2+\frac{3044}{405}\zeta_2^2+\frac{104}{243}\zeta_3\right.\\
&\left.\left.+\frac{19766}{729}\zeta_2+\frac{1865531}{52488}\right)\right].
\end{aligned}
\tag{63}
$$

Finally, we consider the $Hgg$ case. The lower-loop results can be found in [108] as well, and we find from the $Hgg$ form factor $F_g^{(4)}$ in Ref. [65]

$$
\begin{aligned}
C_4^g=&\,C_A^4\left[L^8\left(\frac{1}{24}\right)+L^7\left(\frac{11}{18}\right)+L^6\left(\frac{5}{6}\zeta_2-\frac{119}{162}\right)+L^5\left(-\zeta_3+\frac{22}{9}\zeta_2-\frac{6659}{270}\right)+L^4\left(\frac{181}{20}\zeta_2^2-\frac{187}{18}\zeta_3-\frac{6079}{108}\zeta_2+\frac{30547}{972}\right)\right.\\
&+L^3\left(-16\zeta_5-\frac{46}{3}\zeta_3\zeta_2-\frac{1969}{90}\zeta_2^2-\frac{6511}{81}\zeta_3+\frac{6307}{162}\zeta_2+\frac{391033}{729}\right)+L^2\left(\frac{158}{9}\zeta_3^2+\frac{99791}{1890}\zeta_2^3-\frac{704}{3}\zeta_5+\frac{55}{9}\zeta_3\zeta_2\right.\\
&\left.-\frac{41173}{135}\zeta_2^2+\frac{37027}{243}\zeta_3+\frac{761857}{729}\zeta_2-\frac{1591244}{6561}\right)+L\left(-\frac{2671}{12}\zeta_7-\frac{400}{3}\zeta_5\zeta_2-\frac{307}{5}\zeta_3\zeta_2^2+143\zeta_3^2-\frac{164747}{945}\zeta_2^3\right.\\
&\left.-\frac{63710}{27}\zeta_5+\frac{26983}{27}\zeta_3\zeta_2+\frac{355048}{405}\zeta_2^2+\frac{1763579}{243}\zeta_3-\frac{1989215}{729}\zeta_2-\frac{39280459}{2916}\right)+\left(-\frac{181}{30}\zeta_{5,3}+\frac{2377}{6}\zeta_5\zeta_3\right.\\
&+\frac{271}{9}\zeta_3^2\zeta_2+\frac{4583689}{27000}\zeta_2^4-\frac{224939}{72}\zeta_7+\frac{5423}{6}\zeta_5\zeta_2+\frac{18931}{90}\zeta_3\zeta_2^2+\frac{418801}{162}\zeta_3^2+\frac{353093}{1620}\zeta_2^3+\frac{1203647}{135}\zeta_5\\
&\left.\left.-\frac{1806605}{486}\zeta_3\zeta_2-\frac{778313}{5832}\zeta_2^2-\frac{47586469}{1944}\zeta_3+\frac{32379341}{104976}\zeta_2+\frac{5165679667}{139968}\right)\right]\\
&+\frac{d_A^{abcd}d_A^{abcd}}{N_A}\left[L^2\left(96\zeta_3^2+\frac{1984}{35}\zeta_2^3-\frac{880}{3}\zeta_5-\frac{32}{3}\zeta_3+32\zeta_2\right)+L\left(1742\zeta_7+512\zeta_5\zeta_2-\frac{368}{5}\zeta_3\zeta_2^2-\frac{1672}{3}\zeta_3^2\right.\right.\\
&\left.+\frac{19888}{315}\zeta_2^3+\frac{1360}{9}\zeta_5-1168\zeta_3\zeta_2-\frac{904}{15}\zeta_2^2-\frac{14704}{9}\zeta_3+32\zeta_2+\frac{128}{3}\right)+\left(260\zeta_{5,3}-5092\zeta_5\zeta_3-16\zeta_3^2\zeta_2\right.\\
&-\frac{496766}{525}\zeta_2^4-\frac{6776}{3}\zeta_7-5016\zeta_5\zeta_2+\frac{2992}{3}\zeta_3\zeta_2^2+\frac{31588}{3}\zeta_3^2+\frac{1073972}{945}\zeta_2^3-6460\zeta_5+\frac{6752}{9}\zeta_3\zeta_2+\frac{24616}{45}\zeta_2^2\\
&\left.\left.+\frac{68410}{9}\zeta_3-\frac{4682}{27}\zeta_2-\frac{1310}{9}\right)\right]+n_fC_A^3\left[L^7\left(-\frac{1}{9}\right)+L^6\left(-\frac{43}{81}\right)+L^5\left(-\frac{4}{9}\zeta_2+\frac{379}{45}\right)\right.\\
&+L^4\left(-\frac{91}{9}\zeta_3+\frac{739}{54}\zeta_2+\frac{9245}{486}\right)+L^3\left(\frac{323}{45}\zeta_2^2-\frac{3028}{81}\zeta_3+\frac{64}{3}\zeta_2-\frac{426073}{1458}\right)+L^2\left(-\frac{808}{9}\zeta_5-\frac{178}{9}\zeta_3\zeta_2\right.\\
&\left.+\frac{1202}{15}\zeta_2^2+\frac{2594}{9}\zeta_3-\frac{368554}{729}\zeta_2-\frac{13093133}{26244}\right)+L\left(-46\zeta_3^2+\frac{5726}{135}\zeta_2^3+\frac{7241}{27}\zeta_5+\frac{1028}{27}\zeta_3\zeta_2-\frac{104077}{405}\zeta_2^2\right.\\
&\left.-\frac{445903}{243}\zeta_3+\frac{645433}{729}\zeta_2+\frac{347217971}{34992}\right)+\left(-\frac{8390}{9}\zeta_7+\frac{991}{9}\zeta_5\zeta_2-\frac{2129}{45}\zeta_3\zeta_2^2-\frac{32425}{324}\zeta_3^2-\frac{702253}{5670}\zeta_2^3\right.\\
&\left.\left.+\frac{566977}{540}\zeta_5+\frac{67831}{162}\zeta_3\zeta_2-\frac{2333729}{29160}\zeta_2^2+\frac{9686917}{1944}\zeta_3+\frac{113944685}{104976}\zeta_2-\frac{20463665839}{839808}\right)\right]\\
&+n_fC_A^2C_F\left[L^5\left(\frac{5}{3}\right)+L^4\left(12\zeta_3-\frac{23}{12}\right)+L^3\left(-\frac{16}{5}\zeta_2^2+\frac{728}{9}\zeta_3-\frac{3239}{27}\right)+L^2\left(-\frac{968}{9}\zeta_5+\frac{56}{3}\zeta_3\zeta_2+\frac{64}{45}\zeta_2^2\right.\right.\\
&\left.-\frac{9776}{81}\zeta_3-\frac{1817}{18}\zeta_2+\frac{33560}{243}\right)+L\left(60\zeta_3^2+\frac{3824}{315}\zeta_2^3-\frac{2228}{3}\zeta_5-\frac{3016}{9}\zeta_3\zeta_2+\frac{331}{45}\zeta_2^2-\frac{50758}{27}\zeta_3\right.
\end{aligned}
$$

$$
\begin{aligned}
&+ \frac{9706}{27}\zeta_2 + \frac{7284955}{1944}\Big) + \Big(\frac{16003}{12}\zeta_7 + \frac{230}{9}\zeta_5\zeta_2 - \frac{44}{15}\zeta_3\zeta_2^2 - \frac{1787}{3}\zeta_3^2 + \frac{32254}{945}\zeta_2^3 + \frac{143197}{36}\zeta_5 + \frac{78590}{81}\zeta_3\zeta_2 \\
&- \frac{44839}{540}\zeta_2^2 + \frac{8317937}{1944}\zeta_3 - \frac{293267}{3888}\zeta_2 - \frac{573672965}{46656}\Big)\Big] + n_f C_A C_F^2\Big[L^3\Big(\frac{7}{3}\Big) + L^2\Big(240\zeta_5 - 148\zeta_3 - \frac{116}{3}\Big) \\
&+ L\Big(-40\zeta_3^2 - \frac{160}{7}\zeta_2^3 + \frac{4480}{3}\zeta_5 + \frac{74}{5}\zeta_2^2 - \frac{8084}{9}\zeta_3 - 4\zeta_2 - \frac{6827}{216}\Big) + \Big(-\frac{9580}{3}\zeta_7 - 300\zeta_5\zeta_2 + 12\zeta_3\zeta_2^2 - 368\zeta_3^2 \\
&- \frac{39328}{945}\zeta_2^3 - \frac{92317}{18}\zeta_5 + \frac{193}{3}\zeta_3\zeta_2 - 5\zeta_2^2 + \frac{700879}{108}\zeta_3 - \frac{217}{36}\zeta_2 + \frac{1156175}{1296}\Big)\Big] \\
&+ n_f C_F^3\Big[L(-69) + \Big(3360\zeta_7 - 2940\zeta_5 - 156\zeta_3 + \frac{169}{2}\Big)\Big] + n_f \frac{d_A^{abcd}d_F^{abcd}}{N_A}\Big[L^2\Big(\frac{320}{3}\zeta_5 + \frac{64}{3}\zeta_3 - 64\zeta_2\Big) \\
&+ L\Big(\frac{608}{3}\zeta_3^2 - \frac{7232}{315}\zeta_2^3 - \frac{15440}{9}\zeta_5 + 608\zeta_3\zeta_2 + \frac{1232}{15}\zeta_2^2 + \frac{21248}{9}\zeta_3 - 32\zeta_2 - \frac{608}{3}\Big) + \Big(\frac{2464}{3}\zeta_7 + 1824\zeta_5\zeta_2 \\
&- \frac{1088}{3}\zeta_3\zeta_2^2 - \frac{15700}{3}\zeta_3^2 - \frac{245536}{945}\zeta_2^3 + \frac{108692}{9}\zeta_5 + \frac{1544}{9}\zeta_3\zeta_2 - \frac{35108}{45}\zeta_2^2 - \frac{89932}{9}\zeta_3 + \frac{9580}{27}\zeta_2 + \frac{6944}{9}\Big)\Big] \\
&+ n_f^2 C_A^2\Big[L^6\Big(\frac{8}{81}\Big) + L^5\Big(-\frac{34}{135}\Big) + L^4\Big(-\frac{22}{27}\zeta_2 - \frac{1589}{243}\Big) + L^3\Big(\frac{908}{81}\zeta_3 - \frac{602}{81}\zeta_2 + \frac{34133}{1458}\Big) \\
&+ L^2\Big(-\frac{752}{135}\zeta_2^2 - \frac{3904}{243}\zeta_3 + \frac{626}{9}\zeta_2 + \frac{6162409}{26244}\Big) + L\Big(\frac{344}{9}\zeta_5 - \frac{320}{9}\zeta_3\zeta_2 + \frac{1532}{135}\zeta_2^2 - \frac{51139}{243}\zeta_3 \\
&- \frac{58751}{729}\zeta_2 - \frac{64308517}{34992}\Big) + \Big(\frac{9452}{81}\zeta_3^2 + \frac{15044}{945}\zeta_2^3 - \frac{38071}{135}\zeta_5 + \frac{3113}{486}\zeta_3\zeta_2 + \frac{78953}{3240}\zeta_2^2 + \frac{1103621}{1944}\zeta_3 \\
&- \frac{25105537}{104976}\zeta_2 + \frac{3255482741}{839808}\Big)\Big] + n_f^2 C_A C_F\Big[L^4\Big(-\frac{7}{3}\Big) + L^3\Big(-\frac{160}{9}\zeta_3 + \frac{547}{27}\Big) \\
&+ L^2\Big(\frac{16}{45}\zeta_2^2 - \frac{328}{9}\zeta_3 + \frac{116}{9}\zeta_2 + \frac{5701}{54}\Big) + L\Big(152\zeta_5 + \frac{160}{3}\zeta_3\zeta_2 + \frac{112}{45}\zeta_2^2 + \frac{20200}{27}\zeta_3 - \frac{64}{3}\zeta_2 - \frac{1469381}{972}\Big) \\
&+ \Big(-270\zeta_3^2 - \frac{10084}{945}\zeta_2^3 - \frac{23572}{27}\zeta_5 - \frac{944}{9}\zeta_3\zeta_2 - \frac{764}{135}\zeta_2^2 - \frac{724883}{486}\zeta_3 - \frac{4790}{27}\zeta_2 + \frac{48037931}{11664}\Big)\Big] \\
&+ n_f^2 C_F^2\Big[L^2(4) + L(-320\zeta_5 + 304\zeta_3 - 37) + \Big(\frac{800}{3}\zeta_3^2 + \frac{13696}{945}\zeta_2^3 + \frac{3920}{3}\zeta_5 + \frac{32}{3}\zeta_3\zeta_2 - \frac{212}{15}\zeta_2^2 - 1592\zeta_3 \\
&+ \frac{58}{9}\zeta_2 + \frac{32137}{216}\Big)\Big] + n_f^2\frac{d_F^{abcd}d_F^{abcd}}{N_A}\Big[L\Big(-512\zeta_3 + \frac{704}{3}\Big) + \Big(512\zeta_3^2 - 960\zeta_5 + \frac{384}{5}\zeta_2^2 + 1520\zeta_3 - \frac{9008}{9}\Big)\Big] \\
&+ n_f^3 C_A\Big[L^5\Big(-\frac{4}{135}\Big) + L^4\Big(\frac{20}{81}\Big) + L^3\Big(\frac{16}{27}\zeta_2 + \frac{232}{243}\Big) + L^2\Big(-\frac{16}{3}\zeta_3 - \frac{80}{27}\zeta_2 - \frac{13985}{729}\Big) \\
&+ L\Big(\frac{56}{45}\zeta_2^2 + \frac{2984}{81}\zeta_3 + \frac{64}{81}\zeta_2 + \frac{199244}{2187}\Big) + \Big(-\frac{194}{15}\zeta_5 + \frac{124}{27}\zeta_3\zeta_2 - \frac{944}{405}\zeta_2^2 - \frac{17818}{243}\zeta_3 + \frac{9430}{729}\zeta_2 - \frac{8399887}{52488}\Big)\Big] \\
&+ n_f^3 C_F\Big[L^3\Big(\frac{8}{9}\Big) + L^2\Big(\frac{32}{3}\zeta_3 - \frac{52}{3}\Big) + L\Big(-\frac{32}{45}\zeta_2^2 - \frac{224}{3}\zeta_3 - \frac{40}{9}\zeta_2 + \frac{2936}{27}\Big) + \Big(\frac{640}{27}\zeta_5 - \frac{64}{9}\zeta_3\zeta_2 + \frac{112}{45}\zeta_2^2 \\
&+ \frac{4060}{27}\zeta_3 + \frac{64}{3}\zeta_2 - \frac{233953}{972}\Big)\Big].
\end{aligned}
\tag{64}
$$

In $C_4^q$ and $C_4^{\bar{q}}$, $d_F^{abc}$ is the fully symmetrical tensor originating from the trace over three generators, $N_A$ is the dimension of the adjoint representation, and $n_{q\gamma} = \sum_{q'} Q_{q'}/Q_q$ is the charge-weighted sum over the quark flavors normalized to the charge of the external quark (see Refs. [42,65] for details).

Taking $\mathrm{d}/\mathrm{d}\ln\mu$ of Eqs. (55)–(57) and using the IR structure presented in Eqs. (34)–(40), one can derive a renormalization group equation (RGE) for the hard matching coefficients, which is used to resum logarithms of disparate scales in the SCET framework. The RGE assumes the expected generic form (see, e.g., [109–111])

$$\frac{\mathrm{d}C^r}{\mathrm{d}\ln\mu} = [\Gamma^r(a)L - \gamma^r(a) - 2\mathcal{G}^r]C^r. \tag{65}$$

For a given particle species and color representation the RGE consists of two universal terms related to the renormalization properties of the SCET current, of which the cusp anomalous dimension $\Gamma^r$ controls the leading Sudakov double logarithms, while the collinear anomalous dimension $\gamma^r$ is responsible for resumming single logarithms. The third term $\mathcal{G}^r$, which also governs the single-logarithmic evolution, is related to the anomalous dimension of the QCD current and therefore is nonuniversal. We get $\mathcal{G}^q = 0$ since the vector current is conserved, while for the scalar current this piece reads $\mathcal{G}^b = -(\mathrm{d}\ln Z_m)/(\mathrm{d}\ln\mu^2) = \gamma^m$. For the gluonic case we find quite analogously $\mathcal{G}^g = -(\mathrm{d}\ln Z_\lambda)/(\mathrm{d}\ln\mu^2) = a\mathrm{d}(\beta/a)/\mathrm{d}a$. We checked explicitly that all our matching coefficients satisfy (65) through to four-loop order.

## VI. CONCLUSIONS

In this paper we computed the four-loop corrections to the $Hb\bar{b}$ vertex in massless QCD. Our main result is the analytic expression for the bare form factor presented in Eq. (5). After renormalization of the strong coupling constant and the Higgs-bottom Yukawa coupling, the infrared poles agree with the form predicted in the literature and confirm previous results for the cusp and quark collinear anomalous dimensions. In addition to the new results for the Higgs-bottom form factor, we considered the previously published four-loop results for the bare photon-quark and Higgs-gluon form factors. For all three cases, we employed $Z$ factors to minimally subtract the IR poles from the renormalized form factors, extracted the finite SCET hard matching coefficients, and presented the analytic four-loop results. Our results are available in plain text format in the ancillary files on arXiv.

## ACKNOWLEDGMENTS

A. v. M. and R. M. S. gratefully acknowledge Erik Panzer for related collaborations. This research was supported by the Deutsche Forschungsgemeinschaft (DFG, German Research Foundation) under Grant No. 396021762—TRR 257 “Particle Physics Phenomenology after the Higgs Discovery” and by the National Science Foundation (NSF) under Grant No. 2013859 “Multi-loop amplitudes and precise predictions for the LHC.” The work of A. V. S. and V. A. S. was supported by the Ministry of Education and Science of the Russian Federation as part of the program of the Moscow Center for Fundamental and Applied Mathematics under Agreement No. 075-15-2019-1621. The work of R. N. L. is supported by the Russian Science Foundation, Agreement No. 20-12-00205. We acknowledge the High Performance Computing Center at Michigan State University for computing resources. The Feynman diagrams were drawn with the help of AXODRAW [112] and JAXODRAW [113].

[1] C. Duhr, F. Dulat, and B. Mistlberger, Higgs Boson Production in Bottom-Quark Fusion to Third Order in the Strong Coupling, Phys. Rev. Lett. **125**, 051804 (2020).
[2] C. Duhr, F. Dulat, V. Hirschi, and B. Mistlberger, Higgs production in bottom quark fusion: Matching the 4- and 5-flavour schemes to third order in the strong coupling, J. High Energy Phys. 08 (**2020**) 017.
[3] D. Dicus, T. Stelzer, Z. Sullivan, and S. Willenbrock, Higgs boson production in association with bottom quarks at next-to-leading order, Phys. Rev. D **59**, 094016 (1999).
[4] C. Balazs, H.-J. He, and C. P. Yuan, QCD corrections to scalar production via heavy quark fusion at hadron colliders, Phys. Rev. D **60**, 114001 (1999).
[5] R. V. Harlander and W. B. Kilgore, Higgs boson production in bottom quark fusion at next-to-next-to leading order, Phys. Rev. D **68**, 013001 (2003).
[6] A. H. Ajjath, A. Chakraborty, G. Das, P. Mukherjee, and V. Ravindran, Resummed prediction for Higgs boson production through $b\bar{b}$ annihilation at N$^3$LL, J. High Energy Phys. 11 (2019) 006.
[7] T. Gehrmann and D. Kara, The $Hb\bar{b}$ form factor to three loops in QCD, J. High Energy Phys. 09 (2014) 174.
[8] R. N. Lee, A. V. Smirnov, V. A. Smirnov, and M. Steinhauser, The $N_f^2$ contributions to fermionic four-loop form factors, Phys. Rev. D **96**, 014008 (2017).
[9] S. Dittmaier, M. Krämer, and M. Spira, Higgs radiation off bottom quarks at the Tevatron and the CERN LHC, Phys. Rev. D **70**, 074010 (2004).
[10] S. Dawson, C. B. Jackson, L. Reina, and D. Wackeroth, Exclusive Higgs boson production with bottom quarks at hadron colliders, Phys. Rev. D **69**, 074027 (2004).
[11] M. Wiesemann, R. Frederix, S. Frixione, V. Hirschi, F. Maltoni, and P. Torrielli, Higgs production in association with bottom quarks, J. High Energy Phys. 02 (2015) 132.
[12] D. Pagani, H.-S. Shao, and M. Zaro, RIP $Hb\bar{b}$: How other Higgs production modes conspire to kill a rare signal at the LHC, J. High Energy Phys. 11 (2020) 036.
[13] C. W. Bauer, S. Fleming, and M. E. Luke, Summing Sudakov logarithms in $B \to X_s\gamma$ in effective field theory, Phys. Rev. D **63**, 014006 (2000).
[14] C. W. Bauer, S. Fleming, D. Pirjol, and I. W. Stewart, An effective field theory for collinear and soft gluons: Heavy to light decays, Phys. Rev. D **63**, 114020 (2001).

[15] C. W. Bauer and I. W. Stewart, Invariant operators in collinear effective theory, Phys. Lett. B **516**, 134 (2001).
[16] C. W. Bauer, D. Pirjol, and I. W. Stewart, Soft collinear factorization in effective field theory, Phys. Rev. D **65**, 054022 (2002).
[17] M. Beneke, A. P. Chapovsky, M. Diehl, and T. Feldmann, Soft collinear effective theory and heavy to light currents beyond leading power, Nucl. Phys. **B643**, 431 (2002).
[18] M. Beneke and T. Feldmann, Multipole expanded soft collinear effective theory with nonAbelian gauge symmetry, Phys. Lett. B **553**, 267 (2003).
[19] T. Becher, A. Broggio, and A. Ferroglia, Introduction to soft-collinear effective theory, Lect. Notes Phys. **896**, 1 (2015).
[20] A. H. Mueller, On the asymptotic behavior of the Sudakov form-factor, Phys. Rev. D **20**, 2037 (1979).
[21] J. C. Collins, Algorithm to compute corrections to the Sudakov form-factor, Phys. Rev. D **22**, 1478 (1980).
[22] A. Sen, Asymptotic behavior of the Sudakov form-factor in QCD, Phys. Rev. D **24**, 3281 (1981).
[23] L. Magnea and G. F. Sterman, Analytic continuation of the Sudakov form-factor in QCD, Phys. Rev. D **42**, 4222 (1990).
[24] G. F. Sterman and M. E. Tejeda-Yeomans, Multi-loop amplitudes and resummation, Phys. Lett. B **552**, 48 (2003).
[25] V. Ravindran, J. Smith, and W. L. van Neerven, Two-loop corrections to Higgs boson production, Nucl. Phys. **B704**, 332 (2005).
[26] Z. Bern, L. J. Dixon, and V. A. Smirnov, Iteration of planar amplitudes in maximally supersymmetric Yang-Mills theory at three loops and beyond, Phys. Rev. D **72**, 085001 (2005).
[27] S.-O. Moch, J. A. M. Vermaseren, and A. Vogt, The quark form-factor at higher orders, J. High Energy Phys. 08 (2005) 049.
[28] S. Moch, J. A. M. Vermaseren, and A. Vogt, Three-loop results for quark and gluon form-factors, Phys. Lett. B **625**, 245 (2005).
[29] V. Ravindran, Higher-order threshold effects to inclusive processes in QCD, Nucl. Phys. **B752**, 173 (2006).
[30] L. J. Dixon, L. Magnea, and G. F. Sterman, Universal structure of sub-leading infrared poles in gauge theory amplitudes, J. High Energy Phys. 08 (2008) 022.
[31] T. Becher and M. Neubert, Infrared Singularities of Scattering Amplitudes in Perturbative QCD, Phys. Rev. Lett. **102**, 162001 (2009); Erratum, Phys. Rev. Lett. **111**, 199905 (2013).
[32] T. Becher and M. Neubert, On the structure of infrared singularities of gauge-theory amplitudes, J. High Energy Phys. 06 (2009) 081; Erratum, J. High Energy Phys. 11 (2013) 024.
[33] R. N. Lee, A. V. Smirnov, V. A. Smirnov, and M. Steinhauser, Four-loop quark form factor with quartic fundamental colour factor, J. High Energy Phys. 02 (2019) 172.
[34] R. Brüser, A. Grozin, J. M. Henn, and M. Stahlhofen, Matter dependence of the four-loop QCD cusp anomalous dimension: From small angles to all angles, J. High Energy Phys. 05 (2019) 186.
[35] J. M. Henn, G. P. Korchemsky, and B. Mistlberger, The full four-loop cusp anomalous dimension in $\mathcal{N}=4$ super Yang-Mills and QCD, J. High Energy Phys. 04 (2020) 018.
[36] A. von Manteuffel, E. Panzer, and R. M. Schabinger, Cusp and Collinear Anomalous Dimensions in Four-Loop QCD from Form Factors, Phys. Rev. Lett. **124**, 162001 (2020).
[37] B. Agarwal, A. von Manteuffel, E. Panzer, and R. M. Schabinger, Four-loop collinear anomalous dimensions in QCD and $\mathcal{N}=4$ super Yang-Mills, Phys. Lett. B **820**, 136503 (2021).
[38] C. Anastasiou, F. Herzog, and A. Lazopoulos, The fully differential decay rate of a Higgs boson to bottom-quarks at NNLO in QCD, J. High Energy Phys. 03 (2012) 035.
[39] P. Nogueira, Automatic Feynman graph generation, J. Comput. Phys. **105**, 279 (1993).
[40] J. Kuipers, T. Ueda, J. A. M. Vermaseren, and J. Vollinga, FORM version 4.0, Comput. Phys. Commun. **184**, 1453 (2013).
[41] T. van Ritbergen, A. N. Schellekens, and J. A. M. Vermaseren, Group theory factors for Feynman diagrams, Int. J. Mod. Phys. A **14**, 41 (1999).
[42] R. N. Lee, A. von Manteuffel, R. M. Schabinger, A. V. Smirnov, V. A. Smirnov, and M. Steinhauser, Fermionic corrections to quark and gluon form factors in four-loop QCD, Phys. Rev. D **104**, 074008 (2021).
[43] A. von Manteuffel and C. Studerus, Reduze 2—Distributed Feynman integral reduction, arXiv:1201.4330.
[44] A. von Manteuffel and R. M. Schabinger, A novel approach to integration by parts reduction, Phys. Lett. B **744**, 101 (2015).
[45] J. Gluza, K. Kajda, and D. A. Kosower, Towards a basis for planar two-loop integrals, Phys. Rev. D **83**, 045012 (2011).
[46] K. J. Larsen and Y. Zhang, Integration-by-parts reductions from unitarity cuts and algebraic geometry, Phys. Rev. D **93**, 041701(R) (2016).
[47] J. Böhm, A. Georgoudis, K. J. Larsen, M. Schulze, and Y. Zhang, Complete sets of logarithmic vector fields for integration-by-parts identities of Feynman integrals, Phys. Rev. D **98**, 025023 (2018).
[48] R. N. Lee, Modern techniques of multi-loop calculations, in *Proceedings of the 49th Rencontres de Moriond on QCD and High Energy Interactions: La Thuile, Italy, 2014* (2014), pp. 297–300, arXiv:1405.5616.
[49] T. Bitoun, C. Bogner, R. P. Klausen, and E. Panzer, Feynman integral relations from parametric annihilators, Lett. Math. Phys. **109**, 497 (2019).
[50] B. Agarwal, S. P. Jones, and A. von Manteuffel, Two-loop helicity amplitudes for $gg \to ZZ$ with full top-quark mass effects, J. High Energy Phys. 05 (2021) 256.
[51] A. von Manteuffel, E. Panzer, and R. M. Schabinger, A quasi-finite basis for multi-loop Feynman integrals, J. High Energy Phys. 02 (**2015**) 120.
[52] A. von Manteuffel, E. Panzer, and R. M. Schabinger, On the computation of form factors in massless QCD with finite master integrals, Phys. Rev. D **93**, 125014 (2016).
[53] R. M. Schabinger, Constructing multi-loop scattering amplitudes with manifest singularity structure, Phys. Rev. D **99**, 105010 (2019).

[54] E. Panzer, Algorithms for the symbolic integration of hyperlogarithms with applications to Feynman integrals, Comput. Phys. Commun. **188**, 148 (2015).

[55] F. Brown, The massless higher-loop two-point function, Commun. Math. Phys. **287**, 925 (2009).

[56] F. Brown, On the periods of some Feynman integrals, arXiv:0910.0114.

[57] P. A. Baikov and K. G. Chetyrkin, Four loop massless propagators: An algebraic evaluation of all master integrals, Nucl. Phys. **B837**, 186 (2010).

[58] R. N. Lee, A. V. Smirnov, and V. A. Smirnov, Master integrals for four-loop massless propagators up to transcendentality weight twelve, Nucl. Phys. **B856**, 95 (2012).

[59] A. Kotikov, Differential equations method: New technique for massive Feynman diagrams calculation, Phys. Lett. B **254**, 158 (1991).

[60] Z. Bern, L. J. Dixon, and D. A. Kosower, Dimensionally regulated pentagon integrals, Nucl. Phys. **B412**, 751 (1994).

[61] E. Remiddi, Differential equations for Feynman graph amplitudes, Nuovo Cimento A **110**, 1435 (1997).

[62] T. Gehrmann and E. Remiddi, Differential equations for two loop four point functions, Nucl. Phys. **B580**, 485 (2000).

[63] J. M. Henn, Multi-Loop Integrals in Dimensional Regularization Made Simple, Phys. Rev. Lett. **110**, 251601 (2013).

[64] R. N. Lee, Reducing differential equations for multiloop master integrals, J. High Energy Phys. 04 (2015) 108.

[65] R. N. Lee, A. von Manteuffel, R. M. Schabinger, A. V. Smirnov, V. A. Smirnov, and M. Steinhauser, Quark and Gluon Form Factors in Four-Loop QCD, Phys. Rev. Lett. **128**, 212002 (2022).

[66] T. van Ritbergen, J. A. M. Vermaseren, and S. A. Larin, The four loop beta function in quantum chromodynamics, Phys. Lett. B **400**, 379 (1997).

[67] M. Czakon, The four-loop QCD beta-function and anomalous dimensions, Nucl. Phys. **B710**, 485 (2005).

[68] K. G. Chetyrkin, Quark mass anomalous dimension to $O(\alpha_s^4)$, Phys. Lett. B **404**, 161 (1997).

[69] J. A. M. Vermaseren, S. A. Larin, and T. van Ritbergen, The four loop quark mass anomalous dimension and the invariant quark mass, Phys. Lett. B **405**, 327 (1997).

[70] V. P. Spiridonov, Anomalous dimension of $G_{\mu\nu}^2$ and $\beta$ function, Report No. IYaI-P-0378, 1984.

[71] N. Agarwal, L. Magnea, C. Signorile-Signorile, and A. Tripathi, The infrared structure of perturbative gauge theories, arXiv:2112.07099.

[72] T. Becher and M. Neubert, Infrared singularities of scattering amplitudes and N$^3$LL resummation for $n$-jet processes, J. High Energy Phys. 01 (2020) 025.

[73] S. M. Aybat, L. J. Dixon, and G. F. Sterman, The Two-Loop Anomalous Dimension Matrix for Soft Gluon Exchange, Phys. Rev. Lett. **97**, 072001 (2006).

[74] S. M. Aybat, L. J. Dixon, and G. F. Sterman, The two-loop soft anomalous dimension matrix and resummation at next-to-next-to leading pole, Phys. Rev. D **74**, 074004 (2006).

[75] L. J. Dixon, Matter dependence of the three-loop soft anomalous dimension matrix, Phys. Rev. D **79**, 091501(R) (2009).

[76] E. Gardi and L. Magnea, Infrared singularities in QCD amplitudes, Nuovo Cimento C **32N5-6**, 137 (2009).

[77] E. Gardi and L. Magnea, Factorization constraints for soft anomalous dimensions in QCD scattering amplitudes, J. High Energy Phys. 03 (**2009**) 079.

[78] Ø. Almelid, C. Duhr, and E. Gardi, Three-Loop Corrections to the Soft Anomalous Dimension in Multileg Scattering, Phys. Rev. Lett. **117**, 172002 (2016).

[79] J. M. Henn and B. Mistlberger, Four-Gluon Scattering at Three Loops, Infrared Structure, and the Regge Limit, Phys. Rev. Lett. **117**, 171601 (2016).

[80] F. Caola, A. Chakraborty, G. Gambuti, A. von Manteuffel, and L. Tancredi, Three-loop helicity amplitudes for four-quark scattering in massless QCD, J. High Energy Phys. 10 (2021) 206.

[81] F. Caola, A. Chakraborty, G. Gambuti, A. von Manteuffel, and L. Tancredi, Three-Loop Gluon Scattering in QCD and the Gluon Regge Trajectory, Phys. Rev. Lett. **128**, 212001 (2022).

[82] N. Agarwal, A. Danish, L. Magnea, S. Pal, and A. Tripathi, Multiparton webs beyond three loops, J. High Energy Phys. 05 (2020) 128.

[83] N. Agarwal, L. Magnea, S. Pal, and A. Tripathi, Cwebs beyond three loops in multiparton amplitudes, J. High Energy Phys. 03 (2021) 188.

[84] G. Falcioni, E. Gardi, N. Maher, C. Milloy, and L. Vernazza, Scattering amplitudes in the Regge limit and the soft anomalous dimension through four loops, J. High Energy Phys. 03 (**2022**) 053.

[85] T. Ahmed, M. K. Mandal, N. Rana, and V. Ravindran, Rapidity Distributions in Drell-Yan and Higgs Productions at Threshold to Third Order in QCD, Phys. Rev. Lett. **113**, 212003 (2014).

[86] T. Ahmed, M. K. Mandal, N. Rana, and V. Ravindran, Higgs rapidity distribution in $b\bar{b}$ annihilation at threshold in N$^3$LO QCD, J. High Energy Phys. 02 (2015) 131.

[87] Y. Li, D. Neill, and H. X. Zhu, An exponential regulator for rapidity divergences, Nucl. Phys. **B960**, 115193 (2020).

[88] Y. Li and H. X. Zhu, Bootstrapping Rapidity Anomalous Dimensions for Transverse-Momentum Resummation, Phys. Rev. Lett. **118**, 022004 (2017).

[89] M. A. Ebert, J. K. L. Michel, and F. J. Tackmann, Resummation improved rapidity spectrum for gluon fusion Higgs production, J. High Energy Phys. 05 (2017) 088.

[90] F. Dulat, B. Mistlberger, and A. Pelloni, Precision predictions at N$^3$LO for the Higgs boson rapidity distribution at the LHC, Phys. Rev. D **99**, 034004 (2019).

[91] T. Ahmed, A. H. Ajjath, P. Mukherjee, V. Ravindran, and A. Sankar, Rapidity distribution at soft-virtual and beyond for $n$-colorless particles to N$^4$LO in QCD, Eur. Phys. J. C **81**, 943 (2021).

[92] T. Ahmed, A. H. Ajjath, G. Das, P. Mukherjee, V. Ravindran, and S. Tiwari, Soft-virtual correction and threshold resummation for $n$-colorless particles to fourth order in QCD: Part I, arXiv:2010.02979.

[93] X. Chen, T. Gehrmann, N. Glover, A. Huss, T.-Z. Yang, and H. X. Zhu, Dilepton Rapidity Distribution in Drell-Yan Production to Third Order in QCD, Phys. Rev. Lett. **128**, 052001 (2022).

[94] S. Catani, L. Cieri, D. de Florian, G. Ferrera, and M. Grazzini, Universality of transverse-momentum resummation and hard factors at the NNLO, Nucl. Phys. **B881**, 414 (2014).

[95] T. Becher, G. Bell, C. Lorentzen, and S. Marti, The transverse-momentum spectrum of Higgs bosons near threshold at NNLO, J. High Energy Phys. 11 (2014) 026.

[96] X. Chen, T. Gehrmann, E. W. N. Glover, A. Huss, Y. Li, D. Neill, M. Schulze, I. W. Stewart, and H. X. Zhu, Precise QCD description of the Higgs boson transverse momentum spectrum, Phys. Lett. B **788**, 425 (2019).

[97] D. Gutierrez-Reyes, I. Scimemi, W. J. Waalewijn, and L. Zoppi, Transverse momentum dependent distributions in $e^+e^-$ and semi-inclusive deep-inelastic scattering using jets, J. High Energy Phys. 10 (2019) 031.

[98] D. Gutierrez-Reyes, S. Leal-Gomez, I. Scimemi, and A. Vladimirov, Linearly polarized gluons at next-to-next-to leading order and the Higgs transverse momentum distribution, J. High Energy Phys. 11 (2019) 121.

[99] I. Scimemi and A. Vladimirov, Non-perturbative structure of semi-inclusive deep-inelastic and Drell-Yan scattering at small transverse momentum, J. High Energy Phys. 06 (2020) 137.

[100] G. Billis, B. Dehnadi, M. A. Ebert, J. K. L. Michel, and F. J. Tackmann, Higgs pT Spectrum and Total Cross Section with Fiducial Cuts at Third Resummed and Fixed Order in QCD, Phys. Rev. Lett. **127**, 072001 (2021).

[101] S. Camarda, L. Cieri, and G. Ferrera, Drell–Yan lepton-pair production: $q_T$ resummation at N$^3$LL accuracy and fiducial cross sections at N3LO, Phys. Rev. D **104**, L111503 (2021).

[102] R. Abbate, M. Fickinger, A. H. Hoang, V. Mateu, and I. W. Stewart, Thrust at $N^3LL$ with power corrections and a precision global fit for $\alpha_s(mZ)$, Phys. Rev. D **83**, 074021 (2011).

[103] P. F. Monni, T. Gehrmann, and G. Luisoni, Two-loop soft corrections and resummation of the thrust distribution in the dijet region, J. High Energy Phys. 08 (2011) 010.

[104] J. Gao, Y. Gong, W.-L. Ju, and L. L. Yang, Thrust distribution in Higgs decays at the next-to-leading order and beyond, J. High Energy Phys. 03 (2019) 030.

[105] S. Alioli, A. Broggio, A. Gavardi, S. Kallweit, M. A. Lim, R. Nagar, D. Napoletano, and L. Rottoli, Resummed predictions for hadronic Higgs boson decays, J. High Energy Phys. 04 (2021) 254.

[106] A. H. Ajjath, P. Mukherjee, V. Ravindran, A. Sankar, and S. Tiwari, On next to soft threshold corrections to DIS and SIA processes, J. High Energy Phys. 04 (2021) 131.

[107] M. Abele, D. de Florian, and W. Vogelsang, Threshold resummation at N$^3$LL accuracy and approximate N$^3$LO corrections to semi-inclusive DIS, arXiv:2203.07928.

[108] T. Gehrmann, E. W. N. Glover, T. Huber, N. Ikizlerli, and C. Studerus, Calculation of the quark and gluon form factors to three loops in QCD, J. High Energy Phys. 06 (2010) 094.

[109] T. Becher and M. Neubert, Threshold Resummation in Momentum Space from Effective Field Theory, Phys. Rev. Lett. **97**, 082001 (2006).

[110] V. Ahrens, T. Becher, M. Neubert, and L. L. Yang, Renormalization-group improved prediction for Higgs production at hadron colliders, Eur. Phys. J. C **62**, 333 (2009).

[111] G. Bell, M. Beneke, T. Huber, and X.-Q. Li, Heavy-to-light currents at NNLO in SCET and semi-inclusive $\bar{B} \to X_s l^+ l^-$ decay, Nucl. Phys. **B843**, 143 (2011).

[112] J. A. M. Vermaseren, AXODRAW, Comput. Phys. Commun. **83**, 45 (1994).

[113] D. Binosi and L. Theussl, JAXODRAW: A graphical user interface for drawing Feynman diagrams, Comput. Phys. Commun. **161**, 76 (2004).